$^{40}Ar/^{39}Ar$ ages of CAMP in North America: implications for the Triassic-Jurassic boundary and the ^{40}K decay constant bias.

F. Jourdan [a,b,c*], A. Marzoli [d], H. Bertrand[e], S. Cirilli[f], L. Tanner[g], D. Kontak[h], G. McHone[i], P.R. Renne[a,b], G. Bellieni[d].

[a]*Berkeley Geochronology Center; 2455 Ridge Rd., Berkeley, CA94709, U.S.A.*
[b]*Department of Earth and Planetary Science, University of California, Berkeley, CA94720, U.S.A..*
[c]*Western Australian Argon Isotope Facility; Department of Applied Geology & JdL-CMS, Curtin University of Technology, Perth, WA6845, Australia.*
[d] *Istituto di Geoscienze e Georisorse, CNR, c/o Dipartimento di Geoscienze, Università di Padova, Corso Matteotti, 30, 35137 Padova, Italy*
[e]*UMR-CNRS 5570, Ecole Normale Supérieure de Lyon et Université Claude Bernard, 46, Allée d'Italie, 69364 Lyon, France*
[f]*Dipartimento di Scienze della Terra, Università di Perugia, Piazza Università 1, 06100 Perugia, Italy*
[g]*Department of Biological Sciences, Le Moyne College, Syracuse, NY 13204, U.S.A.*
[h]*Department of Earth Sciences Laurentian University, Sudbury, Ontario, Canada*
[i] *University of Connecticut, Storrs, CT 06268, U.S.A.*

*f.jourdan@curtin.edu.au

Abstract

The Central Atlantic magmatic province (CAMP) is one of the largest igneous provinces on Earth (>10^7 km²) and spanning four continents. Recent high-precision $^{40}Ar/^{39}Ar$ dating of mineral separates has provided important constraints on the age, duration, and geodynamic history of CAMP. Yet, the North American CAMP is strikingly under-represented in this dating effort.

Here we present 13 new statistically robust plateau, mini-plateau and isochron ages obtained on plagioclase and sericite separates from lava flows from the Fundy (n = 10; Nova Scotia, Canada) and Hartford and Deerfield (n = 3; U.S.A.) basins. Ages mostly range from 198.6 ± 1.1 to 200.1 ± 1.4 Ma (2σ), with 1 date substantially younger at 190.6 ± 1.0 Ma. Careful statistical regression shows that ages from the upper (199.7.0 ± 1.5 Ma) and bottom (200.1 ± 0.9 Ma) units of the lava pile in the Fundy basin are statistically indistinguishable, confirming a short duration emplacement (<< 1.8 Ma; ≤1 Ma). Three ages obtained on the Hartford (198.6 ± 2.0 Ma and 199.8 ± 1.1 Ma) and Deerfield (199.3 ± 1.2 Ma) basins were measured on sericite from the upper lava flow units. We interpret these dates as reflecting syn-emplacement hydrothermal activity within these units. Collectively, CAMP ages gathered so far suggest a short duration of the main magmatic activity (2-3 Ma), but also suggest the possibility of a temporal migration of the active magmatic centers from north to south. Such a migration challenges a plume model that would postulate a radial outward migration of the magmatism and is more compatible with other models such as the supercontinent global warming hypothesis. When compared to the age of the Triassic-Jurassic boundary, the filtered CAMP age database suggests that the onset of the magmatic activity precedes the limit by at

least few hundred thousand years, therefore suggesting a causal relationship between CAMP and the end of Triassic mass extinction.
An age at 191 Ma possibly suggests a minor CAMP late tailing activity (190-194 Ma) which has already observed for dykes and sills in Africa and Brazil. We speculate that, if real, this late activity can be due to a major extensional event, possibly heralding the oceanisation process at ~190 Ma. Comparison between high quality U/Pb and $^{40}Ar/^{39}Ar$ ages of pegmatite lenses from the North Mountain basalts confirms a ~1% bias between the two chronometers. This discrepancy is likely attributed to the miscalibration of the ^{40}K decay constants, in particular the electron capture branch.

Keywords: large igneous province; CAMP, $^{40}Ar/^{39}Ar$ ages, magmatic migrations, Triassic Jurassic boundary

Introduction

Many previous studies of large igneous provinces (LIPs) and continental flood basalts (CFBs) have focued on magma composition (e.g. Ingle et al., 2002; Ewart et al., 2004; Deckart et al. 2005; Hou et al., 2006) and the timing of magmatic emplacement (e.g. Baksi & Farrar, 1991; Renne & Basu, 1991; Gurevitch et al., 1995; Courtillot et al., 2000; Coulié et al., 2003;). Although studies concerning the former group are essential to understand the genesis and mantle origin of these giant magmatic provinces, an increasing number of studies of paleomagnetism, and especially absolute geochronology, has provided important constraints on the timing and eruptive rates. Due to the dominance of basaltic rocks in LIPs and CFBs, the $^{40}Ar/^{39}Ar$ technique is the most widely applicable isotopic clock used to investigate these rocks due to its high precision, provided that fresh minerals (mostly plagioclase) have been cautiously selected. Typically, the most significant findings for CFBs concern their origin, geodynamics and timing, relationships with oceanization and possible direct and indirect implications for mass extinctions (cf. Courtillot and Renne, 2003). In addition, geochronology can provide essential information on the giant dyke swarms associated with CFBs, such as their timing and amount of structural inheritance controlling their emplacement (i.e. Jourdan et al., 2006). However, to be considered as reliable, geochronological constraints (and their derived models) must include a sufficient number of data to be statistically valid.
The Central Atlantic Magmatic Province (CAMP) is described as the most extensive CFB on Earth with a surface in excess of 10^7 km², now distributed over four continents (Marzoli et al., 1999; McHone et al., 2005; Fig. 1). Presently, CAMP mostly consists of dykes and sills along with restricted remnants of lava flow sequences preserved in Triassic-Jurassic basins (Olsen et al., 2003). Certainly because of its possible relationship with the onset of the Pangea breakup and the Triassic-Jurassic mass extinction, CAMP is one of the LIPs with the largest number of high-quality (mineral separates) isotopic dates (58 $^{40}Ar/^{39}Ar$ plateau ages obtained so far; cf. filtered compilation by Nomade et al. 2007). Nevertheless, the distribution of the age data in CAMP is far from being homogeneous with, for instance, more than half of the data obtained in Africa. Particularly striking is the scarcity of data (only one age datum available) on the lava flow sequences preserved in the eastern U.S.A. and Canada basins. Such a lack of reliable dates in a crucial area like northwestern CAMP is a significant flaw for any model that aims to understand the global geodynamics of the province or to constrain the age and duration of major lava piles.
Here we investigate the timing of CAMP in eastern North America using the $^{40}Ar/^{39}Ar$ technique on fresh and sericitized plagioclase separates. Our results provide crucial information on the age and duration of the lava piles in the Hartford/Deerfield and Fundy basins. These new ages coupled with the available CAMP age database suggest a brief

emplacement of individual lava piles and that part of the CAMP activity predated the Triassic-Jurassic boundary (TJB) mass extinction. A migration of the magmatic centers throughout the CAMP is also proposed. In addition, our results allow examination of the significance of "sericite" $^{40}Ar/^{39}Ar$ ages as a geochronological tool and further underscore the increasingly documented bias between the $^{40}Ar/^{39}Ar$ and U/Pb ages (Min et al., 2001; Mundil et al., 2006).

Geological setting and previous results.

In this study, we investigated the northwestern part of CAMP rocks that crop out in the Hartford-Deerfield and Fundy basins (Fig. 1 and 2). These basins are part of the eroded remnant of Mesozoic rift basins occurring along the circum- Central Atlantic coasts (from Newfoundland to the Gulf of Mexico; Olsen, 1997; Fig. 1). The basins from Nova Scotia, Canada and the northeastern U.S.A., are termed the Newark Supergroup (Manspeizer and Cousminer, 1988). Their filling sequence includes non-marine Carnian to Early Jurassic sedimentary deposits and the ~ 199 Ma CAMP volcanic sequence (Olsen et al., 2003), which we summarize below.

The Fundy basin

The Fundy basin is the northernmost of the well-exposed Mesozoic rift basins of eastern North America. Most of the basin lies beneath the Bay of Fundy, but the sedimentary strata and volcanics outcrop on the shores of the bay in western Nova Scotia and eastern New Brunswick, ~500 km north of the Hartford basin. In Nova Scotia, the basin is bordered along its northern margin by the Minas Fault Zone, the master fault for the basin (Olsen & Schlische, 1990). The CAMP basalt of the Fundy basin is the North Mountain Basalt, which overlies the Blomidon Formation. The Blomidon Formation (~200-300 m thick) consists of sandstones and mudstones that accumulated mostly in playa, sandflat, eolian and fluvial environments (Tanner, 2000). Based on palynological constraints from one outcrop on the north shore of the Minas Basin (Partridge Island), the TJB has been placed in the uppermost meter of the Blomidon Formation (Fowell and Traverse, 1995; Whiteside et al., 2007) although this was questioned by Tanner et al. (2004) and Lucas and Tanner (2007). On the south shore, the contact between Blomidon sediments and North Mountain Basalt is exposed in generally inaccessible outcrops.
The North Mountain Basalt outcrops occur both on the north shore of the Minas Basin, where it is frequently tectonized, and on the south shore and along the western coast of Nova Scotia where it is only slightly tilted and largely undisturbed. It is not exposed onshore in New Brunswick, but does cover most of Grand Manan Island in the southern Bay of Fundy. The CAMP lava flows reach a thickness of 400 m and can be subdivided into three units. The lower unit (East Ferry Member; up to 185 m thick) consists of a massive basalt lava flow with well developed columnar jointing (Kontak, 2002, 2008) and locally including (upward) coarse-grained feldspar- or pyroxene-rich pegmatite lenses (Papezik et al., 1988; Hodych and Dunning, 1992; Kontak, 2002, 2008). The middle unit (Margaretsville Member) consists of a succession of 10-15 m thick, strongly weathered lava flows, with abundant voids, veins and pipes, generally filled with zeolites (Kontak, 2008). The upper unit (Brier Island Member; up to 150 m thick) is similar to the lower unit and is formed by one or two massive flow(s) with abundant columnar jointing. Rare sedimentary deposits occur locally between the flows of the middle unit, but are otherwise absent within the basaltic sequence. The North Mountain Basalt is overlain by the McCoy Brook Formation. Locally, the carbonate-rich lacustrine strata of the Scots Bay Member rest directly on the surface of the basalt (Tanner, 1996).

Hartford and Deerfield basins

The Hartford Basin and its connected northern extension, the Deerfield Basin (cf. below) are the northernmost of Mesozoic rift basins in the U.S.A. located onshore along the eastern coast (Fig. 1). Both basins are asymmetric half-grabens (Fig. 2a), with the major border fault on the eastern margin of the basins (Hozik et al., 1992) and stratigraphic units dipping eastward (toward the border fault) up to 30°. The Hartford basin fill comprises a succession of four sedimentary and three lava flow formations (Fig. 3; Olsen et al., 2003). From the base to the top, these are: (1) the New Haven Formation mostly consisting of fluvial deposits (~ 2250 m thick). A palynological turnover in the topmost New Haven strata has been interpreted as the Triassic-Jurassic boundary (Olsen et al., 2003); (2) the Talcott Basalt consisting of one to four lava flows, with a total thickness from 65 to 215 m (Puffer et al., 1981); (3) the Shuttle Meadow Formation, which consists of mostly lacustrine deposits with minor fluvio-lacustrine sedimentary rocks (~100 m thick); (4) the Holyoke Basalt that includes two major flows (~100 m thick) and shows locally the presence of coarse-grained evolved segregation sheets (Philpotts et al., 1996); (5) the East Berlin Formation that comprises lacustrine and minor fluvio-lacustrine sedimentary rocks (~150 m thick); (6) the Hampden Basalt (~60 m thick), consisting of one or possibly two moderately to strongly altered lava flows; and (7) the Portland Formation which comprises mostly lacustrine sedimentary rocks in the lower half of the sequence and fluvial sediments in the upper half. Some doleritic dykes thought to be the feeders to the different lava units (based on their geochemical characteristics) crosscut the Hartford basin (Philpotts and Martello, 1986). The most prominent dykes are the Higganum-Holden-Fairhaven dyke, feeder of the Talcott basalts), the Buttress-Ware dyke (feeder of Holyoke basalts) and the Bridgeport-Pelham dyke (feeder of Hampden basalts). Relatively thick sills, e.g. the West Rock sill, can be geochemically correlated to the Talcott lava flows. Samples from these dykes and sills have failed to yield reliable $^{40}Ar/^{39}Ar$ dates so far (F. Jourdan, unpublished data).

The Deerfield basin section is much thinner and includes only three sedimentary formations and one lava flow. The basal formation is the alluvial Sugarloaf Arkose (~2000 m thick), the uppermost portion of which consists of the lacustrine Fall River Beds sequence (~50 m thick). The only basaltic flow in the basin is the Deerfield Basalt. It is ~80 m thick and pervasively altered, mostly affecting the feldspars. Based on the concentrations of immobile elements (e.g., TiO_2) it correlates to the Holyoke Basalt of the Hartford basin (McHone, 1996 and references therein). It is overlain by the fluvial Turners Falls Sandstone and the Mount Toby Conglomerate (~2000 m thick).

The sedimentary and lava flow units of the Hartford-Deerfield basins can be correlated to equivalent formations from the more southern Newark and Culpeper basins, in New Jersey to Virginia (Tollo and Gottfried, 1992; Olsen et al., 2003). In particular, the correspondence of the Talcott Basalt with the Orange Mountain and Mountain Zion Church basalts, respectively, of the Holyoke with the Preakness and Sanders basalt, and of the Hampden Basalt with the Hook Mountain Basalt (Newark basin) is constrained by bio- and cyclo-stratigraphy of the interlayered sediments and by basalt geochemistry, mineralogy and volcanological characteristics.

Prior geochronology of CAMP in North America.

Few reliable $^{40}Ar/^{39}Ar$ and U/Pb dates are available currently for North America CAMP rocks. Carefully statistically filtered $^{40}Ar/^{39}Ar$ age compilations were proposed by Baksi et al. (2003) and by Nomade et al. (2007). The latter compilation will constitute the basis for our

discussion. This compilation excludes K/Ar ages, $^{40}Ar/^{39}Ar$ ages that were obtained on whole rocks (cf. discussion in Jourdan et al., 2007b) and/or using poorly calibrated standards. As a consequence, only 11 ages ranging from 197.5 ± 1.7 to 200.9 ± 1.5 Ma (Hames et al., 2000; Beutel et al., 2005; Nomade et al., 2007) are available. These ages were obtained only on dykes from U.S.A. and no lava flow dates were reliable enough to be included in the CAMP age database (cf. discussion in Nomade et al., 2007). In addition, no $^{40}Ar/^{39}Ar$ ages satisfying the requirements are available for CAMP in Nova Scotia although one recent plateau age was obtained on the North Mountain Basalts (Kontak and Archibald, 2003; recalculated at 200.8 ± 2.2 Ma). However, this age was obtained on whole rock and is rejected from the CAMP $^{40}Ar/^{39}Ar$ age compilation for consistency.

Four U/Pb ages are available for North America. Two of them are from the Gettysburg (201.3 ± 1.0 Ma) and Palisades (200.9 ± 1.0 Ma) sills (Dunning and Hodych, 1990) in U.S.A.. The two other ages are from pegmatitic lenses within the lower unit of the North Mountain basalts. Two multi-grains fractions of zircon yielded ages at 201.7 +1.4/-1.1 Ma (Hodych and Dunning, 1992). Ten single zircon grains yielded a $^{238}U/^{206}Pb$ weighted mean age of 201.3 ± 0.3 Ma (Shoene et al., 2006). Considering the increasingly evidenced -1% age bias of $^{40}Ar/^{39}Ar$ ages due to a slight inaccuracy of the K decay constant (cf. further discussion below), the U/Pb and $^{40}Ar/^{39}Ar$ ages are generally in good agreement.

Sample description and analytical procedures

We selected eleven fresh samples from the Fundy Basin, Nova Scotia. These samples are low-Ti (TiO_2 < 1.7 wt%) tholeiitic basalts (n=9) and pegmatitic gabbros/diorites occurring as segregation sheets in some lava flows (n=2). The primary mineralogy of the basalts consists of augite-pigeonite, plagioclase, Fe–Ti oxides and ±olivine. The pegmatitic segregations are olivine-free and contain interstitial granophyric patches of micropegmatite and apatite needles. Most of the rocks contain slight alteration such as sericite after plagioclase (mostly in cracks). We separated unaltered, optically transparent, 125-200 µm-size, plagioclase of nine of the samples for $^{40}Ar/^{39}Ar$ dating. These minerals were separated using a Frantz magnetic separator, and then carefully hand-picked under a binocular microscope. *Only* completely transparent minerals free of both white cracks (potential reservoirs for sericite) and cloudy regions were selected. In contrast, due to pervasive alteration in the Hampden (Hartford) and Deerfield basalts (U.S.A.), mostly affecting their feldspars, three largely altered low-Ti basaltic samples from these basins were used to obtained strongly/entirely sericitized plagioclase (Annex 1). We selected only white grains, free from visible greenish and brownish inclusions (such as chlorite), in order to estimate the age of hydrothermal alteration events that affected those rocks. After hand-picking, the plagioclase and "sericite" minerals were further leached in diluted HF for one minute and then thoroughly rinsed with distilled water in an ultrasonic cleaner.

One irradiation of 10 h duration (#346FJ) was performed in the Cd-shielded (to minimize undesirable nuclear interference reactions) CLICIT facility of the TRIGA reactor at Oregon State University, U.S.A.. Samples were loaded into large wells of three 1.9 cm diameter and 0.3 cm depth aluminum discs. These wells were bracketed by seven small wells that included Fish Canyon sanidine used as a neutron fluence monitor. We calculated J-values relative to an age of Fish Canyon sanidine of 28.03 Ma (Jourdan and Renne, 2007) and using the decay constants of Steiger and Jager (1977). The three mean J-values computed from the small pits range from 0.0026752 ± 0.0000040 (0.15%) to 0.0026644 ± 0.000054 (0.20%) determined as the average and standard deviation of J-values of the small wells for each irradiation disc. The correction factors for interfering isotopes correspond to the weighted mean of 10 years of measurements of K-Fe and $CaSi_2$ glasses and CaF_2 fluorite in the OSTR reactor: $(^{39}Ar/^{37}Ar)_{Ca}$

= (7.60±0.09)x10^{-4}; (^{36}Ar/^{37}Ar)$_{Ca}$ = (2.70±0.02)x10^{-4}; and (^{40}Ar/^{39}Ar)$_{K}$ = (7.30±0.90)x10^{-4}. ^{40}Ar/^{39}Ar analyses were performed at the Berkeley Geochronology Center using a CO_2 laser. The gas was purified in a stainless steel extraction line using two C-50 getters and a cryogenic condensation trap. Ar isotopes were measured in static mode using a MAP 215-50 mass spectrometer with a Balzers electron multiplier mostly using 10 cycles of peak-hopping. A more complete description of the mass spectrometer and extraction line is given in Renne et al. (1998). Blank measurements were generally obtained before and after every three sample runs. Mass discrimination, assuming a power-law relationship between D and atomic mass, was monitored several times a day (every 9 steps) and provided mean values of 1.00646 ± 0.00238 and 1.00654 ± 0.00248 per dalton (atomic mass unit) depending of the batch of samples analyzed. Ar isotopic data corrected for blank, mass discrimination and radioactive decay are given in Annex 2. Individual errors in Annex 2 are given at the 1σ level. Our criteria for the determination of plateau are as follows: plateaus must include at least 70% of ^{39}Ar. The plateau should be distributed over a minimum of 3 consecutive steps agreeing at 95% confidence level and satisfying a probability of fit of at least 0.05. Plateau ages (Table 1 and Fig. 4) are given at the 2σ level and are calculated using the mean of all the plateau steps, each weighted by the inverse variance of their individual analytical error. Mini-plateaus are defined similarly except that they include between 50% and 70% of ^{39}Ar. Integrated ages (2σ) are calculated using the total gas released for each Ar isotope. Inverse isochrons include the maximum number of consecutive steps with a probability of fit ≥ 0.05. The uncertainties on the ^{40}Ar*/^{39}Ar ratios of the monitors are included in the calculation of the integrated and plateau age uncertainties, but not the errors on the age of the monitor and on the decay constant (internal errors only, see discussion in Min et al., 2000). Detailed ^{40}Ar/^{39}Ar results are shown in Annex 2 and summarized in Table 1.

Mineral major element compositions of sericitized plagioclase from samples HB1 have been analyzed at the IGG-CNR Padova, Italy on a Cameca SX50 electron microprobe (EMP) using ZAF on-line data reduction and matrix correction procedures, at constant accelerating voltage and beam current 15 kV and 15 nA, respectively. Repeated analyses of standards indicate relative analytical uncertainties of about 1% for major and 5% for minor elements. Data are available in Annex 3. Image of the sericitized plagioclase is available in Annex 1.

Results

Eleven samples yielded 10 plateau, 2 mini-plateau and 1 isochron ^{40}Ar/^{39}Ar ages on lava flows from the northeastern U.S.A. (3 analyses) and Nova Scotia (10 analyses on 8 rocks) (Table 1 and Fig. 4). Plateau and mini-plateau ages mostly range from 198.6 ± 1.1 to 201.0 ± 1.4 Ma (2σ), with 1 substantially younger age at 190.6 ± 1.0 Ma.

The northeastern U.S.A. samples (Fig. 1 and 2) yielded three plateau ages on (voluntarily selected) ultra-sericitized plagioclase grains (Annex 1 and 3), as fresh plagioclase grains were too scarce in each sample. We got a plateau age at 199.3 ± 1.2 Ma (MSWD = 0.75; P = 0.77) on the basaltic lava flow unit from the Deerfield basin (HB1). Two other ages at 198.6 ± 2.0 and 199.8 ± 1.1 Ma (MSWD = 1.07 and 1.16 and P = 0.38 and 0.29, respectively) were obtained for samples from lava flows from the Hampden Basalt (HB50 and HB86; Fig. 4 & Table 1) which represents the youngest CAMP flow of the Hartford basin. Due to their K-rich composition, sericitized plagioclase [$KAl_2(OH)_2(AlSi_3O_{10})$] show a Ca/K ratio (~0.1-1; Fig. 4) much lower than usually observed for fresh plagioclase of LIP (e.g. plagioclases from this study show Ca/K ratios varying from ~30 to ~80).

In the Fundy Basin, Nova Scotia, we obtained five plateau ages on the basaltic sequence, sampled at five distinct localities and belonging to the East Ferry (NS3) and Brier Island members (NS9, NS13, NS15, NS21; Fig. 3 and 4; Table 1). These ages range from 201.5 ±

1.1 to 198.9 ± 0.7 Ma (MSWD and P values range from 1.49 to 0.36 and 0.96 to 0.14, respectively). The oldest age from this range (sample NS21) is likely to be affected by cryptic excess ^{40}Ar, as we will discuss later. One sample (NS12) from near the middle of the basaltic sequence (Margaretsville Member) yielded a somewhat perturbed age spectrum with a younger apparent age (Fig. 4). If one outlying step in the middle of the age spectrum is excluded, then a mini-plateau age at 190.6 ± 1.0 Ma (MSWD = 1.6, P = 0.16) is obtained for this sample. The associated Ca/K spectrum is flat therefore suggesting that this plagioclase separate is free of alteration. We believe that this age may be geologically significant, which would imply that NS12 represents a late Later magmatic event, such as a sill (see discussion below). Three plateau ages were obtained on two pegmatitic segregation sheets (NS19 and NS23) sampled near upper part of the East Ferry Member (Fig. 3). On each rock, we analyzed two plagioclase fractions at 150-210 µm and 210-315 µm. Three separates yielded indistinguishable ages ranging from 199.0 ± 1.0 to 199.7 ± 1.0 Ma (MSWD and P values range from 0.93 to 0.10 and 1.00 to 0.49, respectively). The coarser plagioclase fraction of NS23 shows a perturbed bell-shaped spectrum indicating strong ^{40}Ar loss (Fig. 4). It nevertheless gives a mini-plateau age at 197.8 ± 1.0 Ma (MSWD = 0.14; P = 0.98).

We plotted all the results in an inverse isochron diagram for each sample (^{36}Ar/^{40}Ar vs. ^{39}Ar/^{40}Ar not shown; e.g. Heizler and Harrison, 1988). The inverse isochrons yielded apparent ages ranging between 205.9 ± 1.2 and 198.8 ± 1.0 Ma (with the younger age at 192.8 ± 1.6 Ma) concordant with the plateau ages at 2σ (Table 1). Most of the data cluster near the ^{39}Ar/^{40}Ar axis and do not yield meaningful initial ^{40}Ar/^{36}Ar values (64 ± 6 to 330 ± 20; 1σ). In addition, eight analyses (e.g. NS9, NS19) show some evidence of ^{40}Ar loss (± ^{37}Ar recoil and ± recrystallization?) for the low temperature steps with their age spectra following a fickian diffusion profile. Therefore, most of the results do not fulfill the strict definition of an isochron (i.e. a mixing line between trapped and radiogenic ^{40}Ar) which prevents us to use this technique for these samples. Nevertheless, the plateau and "pseudo-isochron" ages are in excellent agreement (Table 1).

One exception is given by sample NS21 and deserves further explanation. This sample shows an integrated age (i.e. the total fusion age; 204.4 ± 2.4 Ma) that is noticeably higher than the plateau age (201.5 ± 1.1 Ma), the latter being older than the isochron age (199.8 ± 1.4 Ma) (Table 1 and Annex 4). Furthermore, this age is older than the otherwise concordant plateau ages obtained for other samples from the upper basalt unit in Nova Scotia (Brier Island member basalt). These observations strongly suggest that NS21 is affected by excess ^{40}Ar*. This is further confirmed by the high initial ^{40}Ar/^{36}Ar value (314 ± 4) obtained by the inverse isochron calculation. Isochrons have been proven a robust technique to derive meaningful ages when excess Ar is present in the sample and when the total ^{40}Ar represents a homogeneous mixing between the excess ^{40}Ar* and the radiogenic ^{40}Ar* produced after the crystallization of the samples (Merrihue and Turner, 1966; Roddick, 1978; Heizler and Harrison, 1988; Sharp and Renne, 2005). The relatively significant spread of NS21 data along the isochron line (Annex 4) allows us to use this technique to calculate a more accurate age for this sample at 199.8 ± 1.4 Ma (MSWD = 1.9; P = 0.05).

Discussion

Age and duration of CAMP in Nova Scotia

Nova Scotia CAMP basalts yielded 4 plateau ages and 1 isochron age ranging from 201.0 ± 1.4 to 198.9 ± 0.7 Ma. Based on their stratigraphic level, the dates belong to the East Ferry (NS3: 200.1 ± 0.9 Ma) and Brier Island members (NS9, NS13, NS15 and NS21: 198.9 ± 0.7

to 201.0 ± 1.4 Ma; Fig. 3). All those ages are statistically quasi-indistinguishable and show no apparent sign of alteration as based on their flat Ca/K spectra.

Deriving a precise duration of the entire sequence using these five ages is not easy because of the relatively large uncertainty on each age and the still low number of analyses. At best, raw standard deviation (2σ) of the five ages and mid-height width of the probability peak (not shown) suggests a duration shorter than 1.6 Ma.

Geological observations can help us to further constrain the emplacement duration of the lava pile. It is not clear if the Brier Island Member consists of a single eruptive event or two lava flows (Kontak, 2002, 2008). The minimum thickness of the member is about 150 m , but we note that the upper contact is not observed. Nevertheless, if we consider the four dates obtained on the Brier Island Member as indicating a single age then we calculate a weighted mean age with an error expanded by student's t time the square root of the MSWD (to account for the scatter of the data) at 199.7 ± 1.5 Ma. The relatively large uncertainty is due to the age scatter which can be attributed to cryptic excess ^{40}Ar* and/or undetected alteration or, admitting that the upper unit includes two lava-flows, the time span between the different eruptive events within the upper units. The total age of the Brier Island Member is then to be compared with the single older age obtained on the East Ferry Member at 200.1 ± 0.9 Ma. These 2 ages are in perfect agreement, though their precision is still too low to derive an absolute duration. Following Jourdan et al. (2007b), we combine analytical treatment and stratigraphic constraints and derive an absolute duration on the North Mountain Basalt lava pile of 0.4 ± 1.7 Ma (2σ).

To conclude, these ages suggest a duration much shorter than 1.6 Ma and most likely on the order of (or shorter than) ~1 Ma, though a more precise estimate is hard to predict with the present dataset. We note however, that more data would be required to allow performing reliable statistical treatment in order to more precisely estimate the North Mountain emplacement duration by radioisotopic techniques (e.g. see for example Hofmann et al., 1997; Jourdan et al.; 2007b).

Two pegmatitic segregations from the East Ferry Member yielded three indistinguishable plateau ages ranging between 199.0 ± 1.0 and 199.7 ± 1.0 Ma (Table 1 and Fig. 4) and a total weighted mean age of 199.4 ± 0.8 Ma. Their ages are similar within error to the ages of the lava flows themselves and confirm the ages obtained for the flow units.

The duration of CAMP volcanism in eastern North America has been estimated using cyclostratigraphy by Olsen et al. (1996; 2003) and Whiteside et al. (2007). According to these authors, the sedimentary layers below, between and above the CAMP lavas (Fig. 3) define a cyclicity controlled by Milankovic climate cycles. Assuming that the preserved sedimentary record is complete and continuous, those cycles can be used to estimate an approximate duration of ~600 ka for the entire lava sequence of the Newark basin (Olsen et al., 2003; Whiteside et al.; 2007). By sedimentary and magnetostratigraphy sequence correlations, they extend this duration to the entire lava sequences located in the multiple North America (including Fundy) and North Africa basins. As discussed by Marzoli et al. (2007) such a time span duration would be correct providing that the sedimentary record is complete. This is questionable to some extent since all the deposit occurs in continental, subaerial environments, and, for instance, the upper Rhaetian (below the first CAMP basalt) may be missing in the Newark basin sequence (Kozur and Weems, 2005; Gallet et al., 2007). Therefore, we interpret the ~600 ka estimates as a *minimum* indicator of the total duration of the Newark and possibly Hartford basin lava piles. However, cyclostratigraphy cannot be applied to the Fundy basin CAMP lava flows because there are no intercalated sedimentary strata. In any case, direct isotopic and analogous cyclostratigraphic ages constrain the duration of the CAMP lava flows in the Fundy basin to between 0.6 and << 1.6 Ma (≤1Ma?).

Age of the Hartford lava and significance of the "sericite" ages.

In tholeiitic CFB sequences, plagioclase is the first-choice mineral for $^{40}Ar/^{39}Ar$ dating but unfortunately it can be partially altered to sericite during subsequent hydrothermal activity. Due to the strong compositional contrast between Ca-rich and K-poor plagioclase of CAMP basalts (K_2O < 0.2 wt%; Jourdan et al., 2003) and sericite (K_2O ~10 wt%), even small amounts of alteration can substantially bias the measured age (Verati and Féraud, 2003; Fuentes et al., 2005). Here, due to the scarcity of fresh plagioclase in all Hampden and Deerfield basalt samples, we choose to select the most altered plagioclase (white "plagioclase" grains almost entirely converted into sericite) in order to date the hydrothermal event(s) in the Hartford and Deerfield basins. We obtained two indistinguishable ages on the Hampden Basalt (upper unit, Fig. 3) at 198.6 ± 2.0 Ma (HB50) and 199.8 ± 1.1 Ma (HB86). A third age at 199.3 ± 1.2 Ma (HB1) is given by the sericite from the Deerfield Basalt (equivalent to the Holyoke Basalt of the Hartford basin; Fig. 3). Ca/K ratios from samples HB86 and HB1 vary between 0.1 and 1, showing almost complete sericitization of the plagioclase grains (Fig. 4). Sample HB50 shows a somewhat higher Ca/K (between 1 and 10, generally) suggesting that the sericitization process was less developed on these plagioclase grains or possibly, but less likely, that the starting Ca/K composition of the plagioclase was substantially higher than for HB86 and HB1. Verati and Féraud (2003) showed that for a typical CFB plagioclase composition (Ca/K ≈ 50), the measured age would approach the age of the hydrothermal event when more than 20% of sericite is present in the separates and would be indistinguishable above 50% of sericitization. A large amount of sericite in the system can produce "alteration" plateau ages as almost all the K comes from the sericite and is no longer influenced by the K content of the pristine plagioclase (e.g. samples B8 and B11 in Jourdan et al., 2003). In other words, tilda-shaped age variation induced by the plagioclase-sericite phase mixture is no longer observed. Additionally, the high K content and alteration origin of the sericite sample prevent any further alteration, rending the K/Ar system quasi-closed to further perturbation.

In the case of the Hartford samples, the sericitization is likely to be largely greater than 50% as suggested by our petrographic observations (Annex 1) microprobe data (Annex 3) and the concordant age spectra. Far from showing a much younger age, however, the ages obtained on the Hartford and Deerfield lava flows are indistinguishable from the peak activity of CAMP derived from fresh plagioclase $^{40}Ar/^{39}Ar$ data on lava flows (this study, Marzoli et al., 1999, 2004; Knight et al. 2004; Nomade et al., 2007; Verati et al. 2007). Accordingly, we interpret these sericite dates as reflecting the hydrothermal activity developed during the cooling of the host flows. This is further justified as the three analyzed samples belong to the topmost Hampden Basalt of the Hartford basin and to the only lava flow of the Deerfield basin, respectively (Fig. 3), excluding subsequent magmatic activity as being responsible for the hydrothermal system. Therefore, and in consideration of the large uncertainties of these dates, which are larger or equal to the total duration of the lava flow sequence, we interpret these ages as representing the emplacement age of the Deerfield and Hampden basalts and their respective synchronous hydrothermal systems.

These three data represent the first reliable ages of CAMP lava flows from Hartford and Deerfield CAMP and are quasi-indistinguishable from the age of Nova Scotia lava flows, although they are potentially slightly younger (cf. discussion below). HB50 and HB86 yield a weighted mean age at 199.5 ± 1.1 Ma (MSWD = 1.1; P = 0.3) for the uppermost formation of the lava pile. This age is statistically indistinguishable from the age at 199.3 ± 1.2 Ma (HB1) obtained on the Deeerfield Basalt, correlated with the Holyoke Basalt, i.e. the middle unit of the Hartford basin (Fig. 3). Calculation of the duration between the top and middle of the lava pile gives a value of 0.2 ± 1.6 Ma (cf. discussion above and Jourdan et al., 2007b) and a 2σ

standard deviation of 1.2 Ma, constraining the duration to be on the order of, or less than, 1.2 Ma. As stated for the Nova Scotia lava pile, this number is likely to be a maximum value and the real duration should be less than 1 Ma. Altogether this suggests that the emplacement time frame of ~70% of the CAMP lava sequence in the Hartford-Deerfield basins is likely to be short, i.e. between 0.3 Ma (Whiteside et al., 2007) and 1.2 Ma (this study). This is similar to our data on the Nova Scotia lava pile and by extension, suggests that the entire sequence emplacement in the Hartford-Deerfield basins is also on the order of (or shorter than) 1 Ma. However, more than three age data would be required to fully verify this hypothesis.

These data are extremely close to the results obtained on 9 CAMP dykes from eastern U.S.A. (Hames et al., 2000; Beutel et al., 2005; Nomade et al., 2007; excluding two ages <195 Ma) that yield a weighted mean age of 198.7 ± 0.3 Ma at 95% confidence level. This mean is noticeably associated with an MSWD of 1.02 and P of 0.42, indicating a very low scatter of the data. Altogether, the lava flows and sills of eastern U.S.A. analyzed so far yield a weighted mean of 198.9 ± 0.3 Ma (MSWD = 1.12; P = 0.34) arguing for a relatively short duration of the CAMP magmatic activity in this region.

Timing of CAMP versus T-J boundary: radioisotopic dating perspective

The Triassic-Jurassic boundary is one of the five largest mass extinctions of the Phanerozoic. Various scenarios have been proposed to explain such a biotic crisis and ultimate causes are still intensively debated. Extensive description of the TJB and possible causes of the crisis are described by Tanner et al. (2004). Among them, the emission of large volumes of volatiles during eruption of the CAMP basalts has been suggested to be a direct or indirect cause of major climate change and mass extinction (Marzoli et al., 1999; Renne & Courtillot, 2003; Marzoli et al., 2004; Tanner et al., 2004, 2007).

In Morocco, the TJB has been proposed by Marzoli et al. (2004 and 2008) to postdate the first CAMP lava-flows therefore suggesting causal relationship between CAMP and the TJB extinction. Detailed biostratigraphic studies by Cirilli et al. (2007) in the Hartford basin yielded similar conclusions, with the TJB revised to be located *above* the Talcott and Holyoke basalts, according to new palynological data on the interlayered sediments (Shuttle Meadow and East Berlin formations). These results are consistent with the described occurrence of Triassic fossils above the lowermost CAMP flows of the Culpeper basin, Virginia (Kozur & Weems, 2005; Lucas & Tanner, 2007).

In the Fundy basin, the TJB has been interpreted as occurring about 30-40 cm below the North Mountain basalt at Partridge Island (North Shore) where the last occurrence of some Triassic palynomorphs has been observed (Fowell and Traverse, 1995; Whiteside et al.., 2007).

Isotopic constraints on the age of the TJB includes a U/Pb single zircon age of 199.6 ± 0.3 Ma obtained on the Sandilands Formation in the Queen Charlotte Islands in western Canada (Pálfy et al., 2000). Considering the ~0.8% bias between $^{40}Ar/^{39}Ar$ and U/Pb chronometers (Mundil et al., 2006), this date is significantly younger than the ages reported throughout CAMP (e.g. Nomade et al., 2007; this study) but careful examination of the data suggests that this age might have suffered from Pb loss and thus might be a minimum age (Mundil & Pálfy, 2005). The more recent estimate of the TJB age is given by an ID-TIMS dating of single chemical-abraded zircon from volcanic ash layers within the Pucara Group, Aramachay Formation in the Utcubamba Valley, northern Peru (Shaltegger et al., 2008). The latter authors obtained an age of 201.6 ± 0.3 Ma, substantially older than the age obtained by Pálfy et al. (2000). This age can be compared with the U/Pb age from a pegmatite lens of the East Ferry Member of the North Mountain Basalt of Nova Scotia (201.3 ± 0.3 Ma; Schoene et al.,

2006), and ~0.8% bias-corrected (Mundil et al., 2006) $^{40}Ar/^{39}Ar$ ages from the East Ferry Member (201.7 ± 1.7 Ma; this study) and CAMP in general (Fig. 5).

U/Pb age vs. U/Pb ages. Comparison between the two U/Pb dates does not need to include error on the decay constant and thus these ages become 201.58 ± 0.17 Ma (TJB in Peru; Schaltegger et al., 2008) and 201.27 ± 0.06 Ma (CAMP pegmatite; Shoene et al., 2006). These two ages are statistically distinguishable with the age obtained on the TJB being 80 to 540 ka older. Schaltegger et al. (2008) discussed the difference between these two ages and proposed that (1) the true age of the TJB might be 75 ka younger on the basis of the stratigraphic constraints (the TJB, as defined by the first appearance of ammonites of the genus Psiloceras, occurs 5 m above the tuff), (2) there is interlaboratory bias, and (3) the pegmatite lens are not the earliest event in the CAMP eruptive sequence, ,but form late in the evolution of the East Ferry Member. We add that the zircon grains obtained from the Aramachay tuff in Peru might include a residence time component of few thousand years (i.e. in this case, the eruption age would be younger than the zircon age). Such residence time effects are increasingly reported for volcanic tuffs and plutons (e.g. Min et al., 2000; Bachmann et al., 2007; Simon et al., 2008) and can matter when the age precision gets as good as few thousand years. In contrast, the formation mode of the North Mountain pegmatite lenses excludes significant residence time, but on the other hand, can include a cooling age component (few tens or hundred ka?; in this case the lava flow emplacement age would be older). We reiterate the conclusion of Schaltegger et al. (2008) that these two ages are not conclusive enough yet for assessing any relationship between CAMP and the TJB.

U/Pb age vs. $^{40}Ar/^{39}Ar$ ages. The advantage of the $^{40}Ar/^{39}Ar$ age over the U/Pb chronometer is that no residence time is affecting K-bearing minerals from volcanic rocks due to their relatively low Ar closure temperatures and that the cooling time of the basaltic lava flow is likely to be instantaneous in contrast to the pegmatite lenses. These gains are however largely balanced by the relatively poor precision of the $^{40}Ar/^{39}Ar$ method compared to the U/Pb technique, especially when the later is measured by ID-TIMS. The age obtained on the lowermost formation of the CAMP in Nova Scotia gives a bias-corrected $^{40}Ar/^{39}Ar$ age of 201.7 ± 1.7 Ma which is clearly not precise enough to give unequivocal information when compared with the U/Pb age of the TJB. *However*, the CAMP database includes to date 69 high-standard statistically filtered mineral separates ages (e.g. Nomade et al., 2007 and this study). When plotted together in a decay-constant-bias-corrected PDD plot, these ages show a gaussian curve centered at ~201 Ma (Fig. 5). The U/Pb age obtained on the TJB plots at the onset of the major eruptive activity and more importantly, several hundred Ka (even Ma) after the onset of the CAMP activity (represented by a statistically significant number of ages; n=15). Altogether these dates confirm biostratigraphic observations in Morroco (Marzoli et al., 2004), Hartford (Cirilli et al., 2007), and Culpeper and Newark (Kozur & Weems, 2005) basins, and measurements of Ir in sediments below the oldest basalts in the Newark and Fundy basins (Tanner and Kyte, 2005) showing that part of CAMP activity predated the TJB. Although the exact volume of this pre-TJB magmatism is still uncertain, the huge total volume of CAMP makes this pre-peak magmatism volumetrically significant. It may have had the potential to initiate substantial climate change, and ultimately generate a large mass extinction.

A possible north to south migration of the magmatism: implications for origin of CAMP

In order to test a possible migration of the magmatic centers during CAMP generation, as previously proposed by Baksi (2003) and Nomade et al. (2007), we calculated the weighted mean (with errors expanded by student's t time the square root of the MSWD) of the statistically filtered $^{40}Ar/^{39}Ar$ ages compiled by Nomade et al. (2007) and the new results from

North America obtained in this study. For this exercise, we consider that the magmatic activity of a given area was brief enough (cf. discussion above on North Mountain Basalt and Hartford-Deerfield lava piles) to be considered as a single date. It should be kept in mind that each of these values represents a mean between the earliest and latest activity of a given area. We regrouped the ages by region (Fig. 1) and we excluded all the ages corresponding to late-stage process (i.e. younger than ~195 Ma).

We obtained weighted mean ages at 95% confidence level of 199.6 ± 0.6 Ma for Nova Scotia (n = 7; MSWD = 2.0; P = 0.05), 198.9 ± 0.3 Ma for eastern U.S.A. (n = 12; MSWD = 1.1; P = 0.34), 198.9 ± 0.5 Ma for Morocco (excluding the slightly younger recurrent lava flow; n=16; MSWD = 0.93; P = 0.53), 198.2 ± 1.3 Ma for Mali (n = 10; MSWD = 7.4; P = 0.00) and 198.0 ± 0.3 Ma for Brazil (n = 7; MSWD = 0.71; P = 0.64) (Fig. 6). Three ages from Guinea yield a weighted mean age of 201 ± 6 Ma with a MSWD of 55, but the low precision and insufficient number of data render this result irrelevant for this exercise. MSWD close to 1 and relatively high probability for each region indicates a low dispersion of the data and argues for a relatively brief emplacement time frame for each area, i.e. likely less than 1 Ma for the main volume.

Two or perhaps three groups of ages arise from this compilation: Nova Scotia basalts would be older (by ~0.7 ± 0.8 Ma) than or synchronous with eastern U.S.A. (and Morroco). A second group (but in fact, possibly the same group), only slightly younger, is given by the CAMP from Morocco and eastern U.S.A. which are a few hundred thousand years younger than Nova Scotia. Indistinguishable mean ages between Morocco and eastern U.S.A. also confirm previous hypotheses based on the geochemistry and magnetostratigraphy (Knight et al., 2004; Marzoli et al., 2004) that proposed that the Moroccan and east-American lava piles have been emitted almost synchronously, although these authors showed that the oldest part of the series (the lower unit of Morocco) is missing in U.S.A..

The CAMP from South America shows a mean age that is ~1.6 ± 0.8 Ma and ~0.9 ± 0.4 Ma younger than CAMP in Nova Scotia and eastern U.S.A., respectively. If calibration between the apparent ages is correct, as implied by the compilation of Nomade et al. (2007), then the age difference between the northern and southern CAMP magmatism is statistically significant. South America has been previously proposed to be the youngest region belonging to the main peak activity of CAMP (Baksi, 2003; Nomade et al., 2007). The relatively low precision on the weighted mean age of CAMP from Mali does not allow distinguishing it from the group Morocco-eastern U.S.A. or Brazil and additional data are urgently required in this region.

The two clearly distinct groups of ages suggest an apparent migration of the magmatism between the northern (Nova Scotia, eastern U.S.A., Morocco) and southern (Brazil) CAMP areas (Fig. 6), or at least temporally distinct magmatic activities throughout the province. These dates support an overall duration of the main magmatic activity of ~2(-3?) Ma (Fig 5), although the peak magmatism of a given region certainly occurred during a much more restricted period (cf. discussion above). Such a migration would challenge the model invoking a mantle plume as the source of CAMP. The plume model postulates that the magma should propagate from the central region of the province, locus of the plume center, toward its margins (e.g. Morgan, 1983; White and McKenzie, 1989; Hill, 1991; Wilson, 1997). Such a plume location has been previously proposed to be centered on the Blake plateau based on an inferred radiating dyke pattern (May., 1971; Hill, 1991; Ernst et al., 1995; Wilson, 1997; Oyarzun et al., 1997; Ernst and Buchan, 2002). However, further studies have demonstrated that part of these dykes follow inherited Proterozoic structures (see discussion in Jourdan et al., 2006) and/or can be Proterozoic in age whether they follow the radial pattern of May (1971) or not (Deckart et al., 1997; Hebeda et al., 1973; Choudhuri et al., 1991; Nomade et al., 2002). An absence of outward migration of the magmatism is in contradiction with the

mantle plume hypothesis as a magma source of CAMP. These results are in accordance with tectonic observations (Tommasi and Vauchez, 2001; DeMin et al., 2003; McHone et al., 2005), elemental and isotopic geochemistry (e.g. Bertrand et al., 1982; Puffer, 2001, 2003; Jourdan et al., 2003; Deckart et al., 2005, Verati et al., 2005) and detailed analysis of regional dyke orientations and distributions (Ragland et al., 1983; McHone, 2000; Verati et al., 2005; McHone et al., 2005; Beutel et al., 2006) that altogether reject the mantle plume hypothesis and favor alternative hypotheses such as shallow mantle melting (Anderson, 1994; Puffer, 2001; Jourdan et al., 2003; Deckart et al., 2005, Verati et al., 2005), most likely triggered by supercontinent "global warming" (Coltice et al., 2007).

A younger event?

Five statistically robust ages that range from 190 to 194 Ma have been previously reported in Guinea (Deckart et al., 1997), Brazil (Baksi and Archibald, 1997; Marzoli et al., 1999; including a whole-rock date) and U.S.A. (Nomade et al., 2007). Two additional ages around 190 Ma have been obtained in Mali (Verati et al., 2005) but were not selected by Nomade et al. (2007) on a statistical basis. Although we agree with the judicious selection of Nomade et al. (2007), the age and Ca/K spectra of these samples do not show any hint of alteration and can be used to support the existence of a possibly significant magmatic event at this time. Here we obtained an additional young age on plagioclase at ~191 Ma. This datum does not show any sign of alteration, though the reason why one step (12% ^{39}Ar) drops by ~10 Ma in the middle of the age spectrum is unknown (Fig. 5). Although this date should not be viewed as a "robust" plateau age to be included in the CAMP age database, it deserves further discussion, in part because of its possible geodynamic implications. This date was obtained on a rock (NS12) sampled within the Margaretsville Member of the North Mountain Basalt, in the Fundy Basin (Fig. 2 and 3). As stressed above, the Brier Island and East Ferry members yielded indistinguishable ages at ~200 Ma, nowhere near 190 Ma. Therefore, we see two possible explanations here: (1) this date is an artifact due to cryptic complications of the K-Ar system or (2) we sampled a sill intruded into the middle unit of the North Mountain Basalt.
Hypothesis (1) cannot be firmly ruled out, though neither is there any sign of alteration visible on the Ca/K ratio (~65; Fig. 4) nor is ^{40}Ar* loss diffusion profile observed on the age spectrum that could explain an anomalously younger age. However, the observed spectrum may have resulted from a resetting of the K-Ar system by a widespread thermal event, around 190 Ma. Such an event is documented by several lines of evidence, in particular the formation of well developed zeolites in the middle basalt unit (Kontak and Archibald, 2003).This NS12 sample has a chemical composition identical to some of the lava flows from the upper unit dated at ~200 Ma (e.g. NS13) which would argue for sub-synchronism for the emplacement of these rocks. Hypothesis (2) is hard to verify as sills and lava flows are difficult to discriminate in the field; however, the site where we collected the massive basalt with fresh plagioclase laths strongly contrasts with the vesiculated and altered middle flow unit observed everywhere else in the North Mountain Basalt and may be an indication that we sampled a sill.
If we admit the validity of the ~191Ma age as a crystallization age (hypothesis 2), it would represent the youngest data obtained so far in North America, providing additional evidence for late scattered activity of CAMP. This tailing activity represents a significant second-order peak in the general CAMP age probability plot (Fig. 5), occurring 7-8 Ma after the peak of the dominant magmatic activity. Despite their younger age, all the rocks investigated so far, that belong to this late magmatic event (Fig. 5) share a low-Ti enriched tholeiitic composition similar to the "common" low-Ti composition that predominates over most of the CAMP. They do not exhibit the MORB affinity which characterizes the late stages of other CFB

provinces like Karoo (Rooi Rand dykes: Duncan et al., 1990; Jourdan et al., 2007a) and Paranà-Etendeka (Horingbaii dyke swarms: Renne et al., 1996). Therefore a sporadic emplacement of enriched lithosphere-derived magmas persisted locally (Nova Scotia, Mali, Guinea, Brazil) until the formation of the first oceanic crust which is inferred to be as old as late Sinemurian (Sahabi et al. 2004), i.e. 190-192 Ma according to the geological timescale of Gradstein et al. (2004). Interestingly, subordinate amounts of CAMP magmas displaying some MORB affinity do occur (e.g. the Hampden basalt in Hartford basin and the recurrent basalt in Morroco) but they do not belong to this late magmatic event.

Some more evidence of a bias in the ^{40}K decay constant

The K/Ar dating technique and its derivative the $^{40}Ar/^{39}Ar$ method are the most versatile techniques as they can measure ages spanning the entire earth and solar system history, from few thousand years up to 4.5 Ga. However, according to recent studies, it emerges that systematic errors associated with the ^{40}K decay constant (Steiger and Jäger, 1977) are now singularly large (e.g. Begemann et al., 2001). More importantly, comparison between $^{40}Ar/^{39}Ar$ and U/Pb ages strongly suggests that the value of ^{40}K decay constant is likely to be slightly off (e.g. Renne et al., 2000; Min et al., 2000; Kwon et al., 2002; Chambers et al., 2005; Villa and Renne, 2005; Krumrei et al., 2006) in particular the electron capture decay branch. This results in U/Pb ages being ~0.8-1% older than $^{40}Ar/^{39}Ar$ ages in the Phanerozoic (Mundil et al., 2006).

Here, our three $^{40}Ar/^{39}Ar$ results on the North Mountain pegmatite lenses offer the possibility to compare them with the recent high-precision single grain zircon U/Pb dates obtained by Schoene et al. (2006) on the same unit (and same sampling site). Schoene et al. (2006) analyzed ten air abraded zircon grains that yielded a $^{238}U/^{206}Pb$ weighted mean age of 201.27 ± 0.06 and ± 0.27 Ma, excluding and including uncertainty of the ^{238}U decay constant, respectively.

Both ages have been obtained using well calibrated standards (Schoene et al., 2006; Jourdan and Renne, 2007) and thus permit a further test of the ^{40}K decay constant bias hypothesis. For the pegmatite lenses, the age difference due to the different closing temperatures of Ar in plagioclase (~150°C) and Pb in zircon (>800°C) (i.e. the cooling ages) is likely to be negligible or at least very short due to the geologically sub-instantaneous crystallization of the pegmatite lenses. Similarly, the residence time of zircon may range from 0 to few thousand years (Kwon et al., 2000; Simon et al., 2008) but can be considered as negligible for Triassic-Jurassic rocks in this exercise. We note that the U/Pb results are obtained on air abraded zircon and *not* using the CA-TIMS technique (Mattison, 2005) that eliminates the zircon domains which have undergone Pb-loss and allows analyzing only closed-system zircon. The Concordia plot of Schoene et al. (2006) suggests that lead loss (along with grain inheritance) is negligible from zircons of the North Mountain pegmatites, and therefore that the zircon age is valid.

We obtained three indistinguishable plateau ages on plagioclase separates that range from 199.0 ± 1.0 to 199.7 ± 1.0 Ma (Table 1 and Fig. 4) and that give a weighted mean age of 199.4 ± 0.9 Ma (with error on J-value propagated on the final weighted mean age). In order to compare our age with U/Pb ages we must include the uncertainties on the age of the FCs monitor (Jourdan and Renne, 2007) and on the current ^{40}K decay constants (Steiger and Jäger, 1977). We recalculate a $^{40}Ar/^{39}Ar$ age of 199.4 ± 1.9 Ma that yields an age difference of -1.9 ± 1.9 Ma (2σ; 1 ± 1 %) with the $^{238}U/^{206}Pb$ age.

As noted by Renne (2000), when all the uncertainties are included in both the $^{40}Ar/^{39}Ar$ and $^{238}U/^{206}Pb$ ages, they are statistically quasi-indistinguishable at 2σ. *However*, the absolute mean values (i.e. 199.4 and 201.3 Ma) between the two systems are offset by ~1%, as

previously observed by Min et al. (2001) on several $^{40}Ar/^{39}Ar$ – U/Pb age couples. Our result thus confirms the existence of a discrepancy between the two geochronometers, most certainly attributed to miscalibration of the ^{40}K decay constants and underscores the necessity to improve both accuracy and precision on the latter using samples with a simple geological history (e.g. Mundil et al., 2006).
Nevertheless it is noteworthy that, although it is problematic to compare $^{40}Ar/^{39}Ar$ and U/Pb ages of the CAMP province due to the bias of ^{40}K decay constant, most of the conclusions concerning the CAMP geochronology (e.g. CAMP emplacement duration and magmatic migrations) are based on the $^{40}Ar/^{39}Ar$ system alone and are thus unaffected by systematic errors carried by the ^{40}K constant as all the ages are shifted by the same amount.

Conclusions

We obtained 10 plateau, 2 mini-plateau and 1 isochron ages on CAMP from Fundy basin (Nova Scotia) and the Hartford and Deerfield basins (U.S.A.) that range from 198.6 ± 1.1 to 201.0 ± 1.4 Ma (2σ), with 1 date substantially younger at 190.6 ± 1.0 Ma. These new results in combination with previous results and geological observations allow drawing the following conclusions:

1. The lava pile of CAMP in the Fundy Basin (North Mountain, Nova Scotia) was emplaced in a very short time span (i.e. << 1.6 Ma and possibly ≤ 1 Ma) at ~200 Ma based on isotopic ages obtained for geologically well-constrained samples from lava flows at the base and the top of the succession.

2. Three ages obtained on sericitized plagioclase grains of basalt lava flows from the Hartford and Deerfield basins (U.S.A.) indicate that hydrothermal alteration is synchronous with the crystallization age of these lava flows and can be used (in conjunction with geological constraints) as a reliable proxy for dating the time of lava extrusion. Age constraints at the middle and top of the sequence suggest a very brief emplacement at ~199 Ma. This age is in perfect accordance with other dates obtained on dykes from eastern U.S.A. and the resulting short duration of CAMP volcanism in this region is consistent with the conclusions of cyclostratigraphic studies of the Newark basin sedimentary successions.

3. Comparison between the ID-TIMS zircon U/Pb age of the Triassic-Jurassic boundary and the CAMP (^{40}K decay-constant bias-corrected) $^{40}Ar/^{39}Ar$ age database shows that the onset of the CAMP magmatic activity precedes the boundary by at least few thousand years, therefore suggesting a causal relationship between CAMP and the Triassic-Jurassic mass extinction. This is in accordance with recent biostratigraphic observations in Morocco and eastern North America sedimentary basins arguing for the Triassic-Jurassic limit occurring within or above the CAMP eruptive sequence.

4. Weighted mean ages calculated for each CAMP region suggest a temporal migration of the magmatic activity with a mean age at 199.6 Ma for Nova Scotia, similar within error to the mean age at 198.9 Ma for eastern U.S.A. and Morocco, but statistically distinct from a ~198 Ma mean age for South America. If these ages are valid, then it implies a 2-3 Ma duration for the main volume of CAMP and provide further evidence against the mantle plume hypothesis in CAMP genesis.

5. A younger age of 190.6 ± 1.0 Ma obtained in Nova Scotia, together with four other young ages (190-194 Ma) reported so far in South America and Africa may suggest the occurrence of a second minor magmatic pulse in the CAMP province. if real, this pulse tapped the same mantle source as the main magmatic peak at ~199 Ma, just prior to or at the same time of the onset of ocean floor spreading.

6. Comparison between zircon U/Pb and plagioclase $^{40}Ar/^{39}Ar$ ages both obtained on the pegmatite lenses of the North Mountain Basalt confirms the previously established bias between the two chronometers. This bias is mostly attributed to the ^{40}K decay constant and in particular the electron capture branch. Miscalibration of the ^{40}K constant shifts the $^{40}Ar/^{39}Ar$ ages by ~ -1% for the Phanerozoic and limits the direct comparison of the $^{40}Ar/^{39}Ar$ and U/Pb database. This study supports an urgent revision of the ^{40}K decay constant.

Acknowledgments

We acknowledge financial support of Padova University (Fondo Ateneo to AM), of the GDR Marges program (INSU-CNRS) from France, the Ann and Gordon Getty Foundation from U.S.A.. T.A. Becker is thanked for analytical assistance. Field work resulting in a new map of the North Mountain Basalt, which formed the basis of our sampling, was supported by funding to D. Kontak from the Nova Scotia Department of Natural Resources.

References

Anderson, D.L., 1994. The sub-lithospheric mantle as the source of continental flood basalts; the case against the continental lithosphere and plume head reservoirs. *Earth and Planetary Science Letters* **123**, 269-280.

Alibert, C., 1985, A Sr-Nd isotope and REE study of the late Triassic dolerites from the Pyrenees (France) and the Messejana dyke (Spain and Portugal), *Earth and Planetary Science Letters 73*, 81-90.

Bachmann, O., Oberli, F. Dungan, M.A., Meier, M. Mundil R. and Fischer H., 2007. $^{40}Ar/^{39}Ar$ and U–Pb dating of the Fish Canyon magmatic system, San Juan Volcanic field, Colorado: Evidence for an extended crystallization history. Chemical Geology 236, 134-166.

Baksi, A.K., 2003. Critical evaluation of $^{40}Ar/^{39}Ar$ ages for the Central Atlantic Magmatic Province; timing, duration and possible migration of magmatic centers. In: Hames, W.E., McHone, J.G., Renne, P.R., Ruppel, C.R. (Eds.), The Central Atlantic Magmatic Province; Insights from Fragments of Pangea. Geophysical Monograph. American Geophysical Union, Washington, pp. 77–90.

Baksi, A.K., Archibald, D.A., 1997. Mesozoic igneous activity in the Maranhão province, northern Brazil: $^{40}Ar/^{39}Ar$ evidence for separate episodes of basaltic magmatism. *Earth and Planetary Science Letters* 151, 139–153.

Begemann, F., Ludwig, K.R., Lugmair, G.W., Min, K., Nyquist, L.E., Patchett, P.J., Renne, P.R., Shih, C.-Y., Villan, I.M., Walker, R.J., 2001. Call for an improved set of decay constants for geochronological use, *Geochimica et Cosmochimica Acta* **65**, 111-121.

Benson, R.M., 2003. Age estimates of the seaward dipping volcanic wedge, earliest oceanic crust, and earliest drift-stage sediments along the North Atlantic margin. In: Hames, W.E., McHone, J.G., Renne, P.R., Ruppel, C.R. (Eds.), The Central Atlantic Magmatic

Province; Insights from Fragments of Pangea. American Geophysical Union, Washington, pp. 61–75.

Bertrand, H., Dostal, J., Dupuy, C., 1982. Geochemistry of early Mesozoic tholeiites from Morocco. *Earth and Planetary Science Letters* 58, 225–239.

Bertrand, H., 1991. The Mesozoic Tholeiitic Province of Northwest Africa: a volcano-tectonic record of the early opening of Central Atlantic. In: Kampunzu, A.B., Lubala, R.T. (Eds.), Magmatism in Extensional Structural Settings. The Phanerozoic African Plate. Springer-Verlag, Berlin, pp. 147–188.

Beutel, E.K., Nomade, S., Fronabarger, A.K., Renne, P.R., 2005. Pangea's complex break-up: new Mesozoic dike and $^{40}Ar/^{39}Ar$ dates. *Earth and Planetary Science Letters* 236, 471–485.

Cebria, J.M., Lopez-Ruiz, J., Doblas, M., Martins, L.T., Munha, J., 2003. Geochemistry of the early Jurassic Messejana-Plasencia dyke (Portugal–Spain); implications on the origin of the Central Atlantic Magmatic Province. Journal of Petrology 44, 547–568.

Chambers, L.M., Pringle, M.S., Parrish, R.R. 2005. Rapid formation of the Small Isles Tertairy centre constrained by precise $^{40}Ar/^{39}Ar$ and U-Pb ages. *Lithos*, **79**, 367-384

Choudhuri, A., Oliveira, E.P., Sial, A.N., 1991. Mesozoic dyke swarms in northern Guiana and northern Brazil and the Cape Verde-Fernando de Noronha Vortices: a synthesis. International symposium of Mafic Dykes, Sao Paulo, Brazil, pp. 17–22.

Cirilli, S., Marzoli, A., Tanner, L., Bertrand, H., Jourdan, F., Bellieni, G., 2007. Stratigraphic constrains for the age of CAMP volcanism and its relationship with the T-J climatic and biotic crisis. GeoItalia conference abstract, Rimini, Italia.

Coltice, N., Phillips, B.R., Bertrand, H., Ricard, Y., Rey, P., 2007. Global warming of the mantle at the origin of flood basalts over supercontinents. Geology 35, 391-394.

Coulié, E., Quidelleur, X., Gillot, P.-Y., Courtillot, V., Lefèvre, J.-C., Chiesa S., 2003, Comparative K–Ar and Ar/Ar dating of Ethiopian and Yemenite Oligocene volcanism: implications for timing and duration of the Ethiopian traps, *Earth and Planetary Science Letters* 206, 477–492.

Courtillot, V., Gallet, Y., Rocchia, R., Féraud, G., Robin, E., Hofmann, C., Bhandari, N., Ghevariya, Z.G. 2000. Cosmic markers, $^{40}Ar/^{39}Ar$ dating and paleomagnetism of the KT sections in the Anjar area of the Deccan large igneous province, *Earth and Planetary Science Letters* 182, 137–156.

Courtillot, V., Renne, P.R., 2003. On the ages of flood basalt events. Comptes Rendus des Geosciences 335, 113–140.

De Min, A., Piccirillo, E.M., Marzoli, A., Bellieni, G., Renne, P.R., Ernesto, M., Marques, L.S., 2003. The Central Atlantic Magmatic Province (CAMP) in Brazil; petrology, geochemistry, $^{40}Ar/^{39}Ar$ ages, paleomagnetism and geodynamic implications. In: Hames, W.E., McHone, J.G., Renne, P.R., Ruppel, C.R. (Eds.), The Central Atlantic Magmatic Province; Insights from Fragments of Pangea: Geophysical Monograph. American Geophysical Union, Washington, pp. 91–128.

Deckart, K., Feraud, G., Bertrand, H., 1997. Age of Jurassic continental tholeiites of French Guyana, Suriname, and Guinea: implications for the initial opening of the Central Atlantic Ocean. *Earth and Planetary Science Letters* 150, 205–220.

Deckart, K., Bertrand, H., Liegeois, J.P., 2005. Geochemistry and Sr, Nd, Pb isotopic composition of the Central Atlantic Magmatic Province (CAMP) in Guyana and Guinea. Lithos 82, 289–314.

Duncan A. R., Armstong R.A., Erlank, A.J., Marsh, J.S & Watkins, R.T., 1990. MORB-related dolerites associated with the final phases of Karoo flood basalt volcanism in southern Africa. In A. J. Parker, Rickwood, P.C., Tucker, D.H. (Eds) *Mafic dykes and emplacement mechanisms*. Rotterdam: Balkema, 119-129.

Dunn, A.M., Reynolds, P.H., Clarke, D.B., Ugidos, J.M., 1998. A comparison of the age and composition of the Shelburne dyke, Nova Scotia, and the Messejana dyke, Spain. Canadian Journal of Earth Sciences 35, 1110–1115.

Dupuy, C., Marsh, J., Dostal, J., Michard, A., Testa, S., 1988. Asthenospheric and lithospheric sources for Mesozoic dolerites from Liberia (Africa): trace element and isotopic evidence. *Earth and Planetary Science Letters* 87, 100– 110.

Dunning, G.R., Hodych, J.P., 1990. U/Pb zircon and baddeleyite ages for the Palisades and Gettysburg sills of the northeastern United States: implications for the age of the Triassic/Jurassic boundary. Geology 18, 795–798.

Ernst, R.E., Head, J.W., Parfitt, E., Grosfils, E., Wilson, L., 1995. Giant radiating dyke swarms on Earth and Venus. Earth Science Review 39, 1–58.

Ernst, R.E., Buchan, K.L., 2002. Maximum size and distribution in time and space of mantle plumes: evidence from large igneous provinces. Journal of Geodynamics 31, 309– 342.

Fowell, S.J., Traverse, A., 1995. Palynology and age of the upper Blomidon Formation, Fundy basin, Nova Scotia. Review of Paleobotanic and Palynolgy 86, 211 –233.

Fuentes, F. Féraud, G., Aguirre, L., Morata, D., 2005. $^{40}Ar/^{39}Ar$ dating of volcanism and subsequent very low-grade metamorphism in a subsiding basin: example of the Cretaceous lava series from central Chile. Chemical Geology 214, 157-177.

Gallet, Y., Krystyn, L., Marcoux, J., Besse, J., 2007. New constraints on the End-Triassic (Upper Norian–Rhaetian) magnetostratigraphy. Earth and Planetary Science Letters 255, 458-470.

Gradstein F.M., Ogg, J.G., Smith, A.G. et al., 2004. A geological time Scale 2004. International commission on Stratigraphy (ICS) available at www.stratigraphy.org.

Gurevitch, E., Westphal, M., Daragan-Suchov, J., Feinberg, H., Pozzi, J.-P., Khramov, A.N., 1995. Paleomagnetism and magnetostratigraphy of the traps from western Taymir (northern Siberia) and the Permo-Triassic crisis, Earth and Planetary Science Letters 136, 461–473.

Hames, W.E., Renne, P.R., Ruppel, C.R., 2000. New evidence for geologically instantaneous emplacement of earliest Jurassic Central Atlantic magmatic province basalts on the North American margin. Geology 28, 859–862.

Hebeda, E.H., Boelrijk, N.A.I.M., Priem, H.N.A., Verdurmen, E.A.T., Verschure, R.H., 1973. Excess radiogenic argon in the Precambrian Avanavero Dolerite in western Surinam (South America). Earth and Planetary Science Letters 20, 189–200.

Heizler M.T., Harrison, T.M., 1988. Multiple trapped argon isotope components revealed by $^{40}Ar/^{39}Ar$ isochron analysis. *Geochimica et Cosmochimica Acta* **52**, 1295-1303.

Hill, R.I., 1991. Starting plume and continental break-up, Earth and Planetary Science Letters, 398-416.

Hodych, J.P., Dunning, G.R., 1992. Did the Manicouagan impact trigger end-of-Triassic mass extinction? Geology 20, 51–54.

Hofmann, C., Courtillot, V., Féraud, G., Rochette, P., Yirgu, G., Dtefo, E., and Pick, R., 1997. Timing of the Ethiopian flood basalt event and implications for plume birth and global change: Nature, v. 389, p. 838–841, doi: 10.1038/39853.

Hou, Z.Q., Lu J.R., Lin S.Z., 2006. Heterogeneity of a plume axis: Bulk-rock geochemical evidence from picrites and basalts in the Emeishan large igneous province, southwest China. International Geology Review 48, 1087-1112.

Hozik, M.J., 1992. Paleomagnetism of igneous rocks in the Culpeper, Newark, and Hartford/Deerfield basins. In: Puffer, J.H., Ragland, P.C. (Eds.), Eastern North American Mesozoic Magmatism. Geological Society of America Special Paper, vol. 268, pp. 279–308.

Ingle, S., Weis, D., Scoates, J.S., Frey, F.A., 2002. Relationship between the early Kerguelen plume and continental flood basalts pf the paleo-Eastern Gondwanan margins, Earth and Planetary Science Letters 197, 35–50.

Janney, P.E., Castillo, P.R., 2001. Geochemistry of the oldest Atlantic oceanic crust suggests mantle plume involvement in the early history of the Central Atlantic Ocean. Earth and Planetary Science Letters 192,291–302.

Jourdan, F., Marzoli, A., Bertrand, H., Cosca, M., Fontignie, D., 2003. The northernmost CAMP; $^{40}Ar/^{39}Ar$ age, petrology and Sr–Nd–Pb isotope geochemistry of the Kerforne Dike, Brittany, France. In: Hames, W.E., McHone, J.G., Renne, P.R., Ruppel, C.R. (Eds.), The Central Atlantic Magmatic Province; Insights from Fragments of Pangea: Geophysical Monograph. American Geophysical Union, Washington, pp. 209–226.

Jourdan, F., Féraud, G., Bertrand, H., Watkeys, M.K., 2007a. From flood basalts to the onset of oceanisation: example from the $^{40}Ar/^{39}Ar$ high-resolution picture of the Karoo large igneous province, Geochemistry Geophysics Geosystems 8, Q02002.

Jourdan, F., Féraud, G., Bertrand, H., Watkeys, M.K., Renne, P.R., 2007b. Distinct brief major events in the Karoo large igneous province clarified by new $^{40}Ar/^{39}Ar$ ages on the Lesotho basalts. Lithos 98, 195-209.

Jourdan, F. and Renne, P.R., 2007. Age calibration of the Fish Canyon sanidine $^{40}Ar/^{39}Ar$ dating standard using primary K-Ar standards. Geochimica et Cosmochimica Acta 71, 387-402.

Klitgord, K.D. Schouten, H. Plate kinematics of the Central Atlantic, in: P.R. Vogt, B.E. Tucholke (Eds.), The Western North Atlantic Region, The Geology of North America, Geological Society of America, 1986, pp. 351–377.

Knight, K.B., Nomade, S., Renne, P.R., Marzoli, A., Bertrand, H., Youbi, N., 2004. The Central Atlantic Magmatic Province at the Triassic–Jurassic boundary: paleomagnetic and $^{40}Ar/^{39}Ar$ evidence from Morocco for brief, episodic volcanism. Earth and Planetary Science Letters 228, 143–160.

Kontak, D.J., 2002. Internal stratigraphy of the Jurassic North Mountain Basalt, southern Nova Scotia. In:MacDonald, D.R. (Ed.), Mines and Minerals Branch Report of Activities 2001. Nova Scotia Department of Natural Resources, Report 2002-1, pp. 69–79.

Kontak, D.J., Archibald, D.A., 2003. $^{40}Ar/^{39}Ar$ age of the Jurassic North Mountain Basalt, southwestern Nova Scotia. Atlantic Geology 39, 47-53.

Kontak, D.J., 2008. On the edge of CAMP: Geology and volcanology of the Jurassic North Mountain Basalt, Nova Scotia. *Lithos* **101**, 74-101.

Kozur, H. and Weems, R. Conchostracan evidence for a late Thaetian to Early Hettangian for the CAMP volcanic event in the Newark Supergroup, and a Sevaian (late Norian) age for the immediately underlying beds, Hallesches Jahrb. Geowiss. B27 (2005), pp. 21–51.

Krumrei T.V., Villa, I.M., Marks, M.A.W., Markl, G., 2006. A $^{40}Ar/^{39}Ar$ and U/Pb isotopic study of the Ilimaussaq complex, South Greenland: implication of the ^{40}K decay constant and for the duration of magmatic activity in peralkaline complex. *Chemical Geology* **227**, 258-273.

Kwon J., Min, K., Bickel, P., Renne, P.R., 2002. Statistical methods for jointly estimating decay constant of 40K and age of a dating standard. *Mathematic Geology* **175**, 457-474.

Manspeizer, W., Cousminer, H.L.. Late Triassic-Early Jurassic synrift basins of the U.S. Atlantic margin. in Sheridan R.E., and Grow J.A. Eds., The Geology of North America, vol I-2 (1988),197-216. The Atlantic Continental Margin, U.S.: Geological Society of America

Marzoli, A., Renne, P.R., Piccirillo, E.M., Ernesto, M., Bellieni, G., De Min, A., 1999. Extensive 200-million-year-old continental flood basalts of the Central Atlantic Magmatic Province. Science 284, 616–618.

Marzoli, A., Bertrand, H., Knight, K.B., Cirilli, S., Buratti, N., Vérati, C., Nomade, S., Renne, P.R., Youbi, N., Martini, R., Allenbach, K., Neuwerth, R., Rapaille, C., Zaninetti, L., Bellieni, G., 2004. Synchrony of the Central Atlantic magmatic province and the Triassic–Jurassic boundary climatic and biotic crisis. Geology 32, 973–976.

Marzoli, A., Bertrand, H., Knight, K., Cirilli, S., Nomade, S., Renne, P.R., Vérati, C., Youbi, N., Martini, R., Bellieni G., 2008 Synchrony between the Central Atlantic magmatic province and the Triassic-Jurassic mass-extinction event? Comment. Palaeogeography, Palaeoclimatology, Palaeoecology, 262, 189-193.

Mattison, J.M., 2005. Zircon U-Pb chemical-abrasion (CA-TIMS) method: combined annealing and multi-step dissolution analysis for improved precision and accuracy of zircon ages. *Chemical Geology* **220**, 47-66.

May, P.R., 1971. Patterns of Triassic diabase dikes around the North Atlantic in the context of predrift position of the continents. Geological Society of America Bulletin 82, 1285–1292.

McHone, J.G., 1996. Broad-terrane Jurassic flood basalts across northeastern North America. Geology 24, 319–322.

McHone, J.G., 2000. Non-plume magmatism and rifting during the opening of the Central Atlantic Ocean. Tectonophysics 316, 287–296.

McHone, J.G., Anderson, D.L., Beutel, E.K., and Fialko, Y.A., 2005, Giant dikes, rifts, flood basalts, and plate tectonics: A contention of mantle models, in Foulger, G.R., Natland, J.H., Presnall, D.C., and Anderson, D.L., eds., Plates, plumes, and paradigms: Geological Society of America Special Paper 388, p. 401–420

Merrihue C., Turner, G., 1966. Potassium-argon dating by activation with fast neutrons. *Journal of Geophysical Research* **71**, 2852-2857.

Min, K., Mundil, R., Renne, P.R., Ludwig, K.R., 2000. A test for systematic errors in $^{40}Ar/^{39}Ar$ geochronology through comparison with U–Pb analysis of a 1.1 Ga rhyolite. Geochimica Cosmochimica Acta 64, 73–98.

Morgan, W.J., 1981. Hotspot tracks and the opening of the Atlantic and Indian Ocean. In: C. Emiliani (Eds), *The sea. volume 7: The Oceanic Lithosphere*. New York: Wiley.

Mundil, R., Renne, P.R., Min, K., Ludwig, K.R., 2006. Resolvable miscalibration of the geochronometer, Eos Trans. AGU, 87(52), Fall Meeting Supplementary, Abstract V21A-0543.

Mundil, R., Pàlfy, J., 2005. Triassic-Jurassic time scale and mass extinction: Current status and new constraints, Geochimica et Cosmochimica Acta 69, A320.

Nomade, S., Pouclet, A., Chen, Y., 2002. The French Guyana doleritic dykes: geochemical evidence of three populations and new data for the Jurassic Central Atlantic Magmatic Province. Journal of Geodynamics 34, 595–614.

Nomade, S., Renne, P.R., Merkle, R.K.W., 2004. $^{40}Ar/^{39}Ar$ age constraints on ore deposition and cooling of the Bushveld Complex, South Africa. Journal of the Geological Society of London, 161, 411-420.

Nomade, S, Knight, K.B., Beutel, E., Renne, P.R., Vérati, C., Féraud, G., Marzoli, A., Youbi N., Bertrand, H., 2007. Chronology of the Central Atlantic Magmatic Province: Implications for the Central Atlantic rifting processes and the Triassic–Jurassic biotic crisis. Palaeogeography, Palaeoclimatology, Palaeoecology 246, 326-344.

Olsen, P.E., 1997. Stratigraphic record of the early Mesozoic breakup of Pangea in the Laurasia-Gondwana rift system. Annual Review of Earth Planetary Sciences 25, 337–401.

Olsen, P.E., Schlische, R.W., 1990. Transtensional arm of the early Mesozoic Fundy rift basin: penecontemporaneous faulting and sedimentation, Geology 18, 695– 698.

Olsen, P.E., Schlische, R.W., Fedosh, M.S., 1996. 580 ky duration of the Early Jurassic flood basalt event in eastern North America estimated using Milankovitch cyclostratigraphy. In:

Morales, M. (Ed.), The Continental Jurassic, Museum of Northern Arizona Bulletin, vol. 60, pp. 11–22.
Olsen, P.E., 1999. Giant lava flows, mass extinctions, and mantle plumes. Science 284, 604-605.
Olsen, P.E., Kent, D.V., Et-Touhami, M., Puffer, J.H., 2003. Cyclo-, magneto-, and bio-stratigraphic constraints on the duration of the CAMP event and its relationship to the Triassic–Jurassic boundary. In: Hames, W.E., McHone, J.G., Renne, P.R., Ruppel, C.R. (Eds.), The Central Atlantic Magmatic Province; Insights from Fragments of Pangea: Geophysical Monograph. American Geophysical Union, Washington, pp. 7–32.
Onstott T.C., Miller M.L., Ewing R.C., and Walsh, D., 1995. Recoil refinements: Implications for the $^{40}Ar/^{39}Ar$ dating technique. *Geochim. Cosmochim. Acta* **59**, 1821-1834.
Oyarzun, R., Doblas, M., Lopez-Ruiz, J., Cebria, J.M., 1997. Opening of the Central Atlantic and asymmetric mantle upwelling phenomena: implications for long lived magmatism in western North Africa and Europe. Geology 27, 727–730.
Pàlfy, J., Mortensen, J.K., Carter, E.S., Smith, P.L.,Friedman, R.M., and Tipper, H.W., 2000, Timing the end-Triassic mass extinction: First on land, then in the sea?: Geology 28, 39-42.
Papezik, V.S., Greenough, J.D., Colwell, J.A., Mallinson, T.J., 1988. North Mountain Basalt from Digby, Nova Scotia; models for a fissure eruption from stratigraphy and petrochemistry. Canadian Journal of Earth Sciences 25, 74-83.
Pe-Piper, G., Reynolds, P.H., 2000. Early Mesozoic alkaline mafic dykes, southwestern Nova Scotia, Canada, and their bearing on Triassic–Jurassic magmatism. Canadian Mineralogist 38, 217–232.
Pegram,W.J., 1990. Development of continental lithospheric mantle as reflected in the chemistry of the Mesozoic Appalachian Tholeiites, U.S.A.. Earth and Planetary Science Letters 97, 316– 331.
Philpotts, A.R., Martello, A., 1986. Diabase feeder dikes for Mesozoic basalts in southern New England. American Journal of Science 96, 1131–1139.
Philpotts, A.R. 1998. Nature of a flood-basalt-magma reservoir based on the compositional variation in a single flood-basalt flow and its feeder dike in the Mesozoic Hartford Basin, Connecticut. Contributions to Mineralogy and Petrology 133, 69-82.
Philpotts, A.R., Carrol, M., Hill., 1996. Crystal-Mush Compaction and the Origin of Pegmatitic Segregation Sheets in a Thick Flood-Basalt Flow in the Mesozoic Hartford Basin, Connecticut. Journal of Petrology 37, 811 - 836.
Puffer, J.H., 2001. Contrasting high field strength element contents of continental flood basalts from plume versus reactivated-arc sources. Geology 29, 675– 678.
Puffer, J.H., 2003. A reactivated back-arc source for CAMP magma. In: Hames, W.E., McHone, J.G., Renne, P.R., Ruppel, C.R. (Eds.), The Central Atlantic Magmatic Province; Insights from Fragments of Pangea: Geophysical Monograph. American Geophysical Union, Washington, pp. 151–162.
Puffer, J.H., Hurtubise, D.O., Geiger, F.J., Lechler, P., 1981. Chemical-composition and stratigraphic correlation of Mesozoic basalt units of the Newark Basin, New-Jersey, and the Hartford basin, Connecticut – Summary. Geological Society of America Bulletin 92, p155-159.
Ragland, P.C., Hatcher, R.D.Jr, Whittington, D., 1983. Juxtaposed Mesozoic diabase dike sets from the Carolinas; a preliminary assessment. Geology 11, 394-399.
Reichow, M.K., Saunders, A.D., White, R.V., Pringle, M.S., Al'Mukhamedov, A.I., Medvedev, A.I., Kirda, N.P., 2002. Ar-40/Ar- 39 dates from the West Siberian Basin: Siberian flood basalt province doubled, Science 296, 1846–1849.

Renne, P.R., Glen, J.M., Milner, S.C., Duncan, A.R., 1996. Age of Etendeka flood volcanism and associated intrusions in southwestern Africa, *Geology 24*, 659-662.

Renne, P.R., Swisher III, C.C., Deino, A.L., Karner, D.B., Owens, T., DePaolo, D.J., 1998. Intercalibration of standards, absolute ages and uncertainties in 40Ar/39Ar dating. Chemical Geology 145, 117–152.

Renne, P.R., 2000. $^{40}Ar/^{39}Ar$ age of plagioclase from Acapulco meteorite and the problem of systematic errors in cosmochronology. Earth and Planetary Science Letters 175, 13–26.

Roddick, J.C., 1978. The application of isochron diagrams in ^{40}Ar-^{39}Ar dating; a discussion. Earth and Planetary Science Letters **41**, 233-244.

Rossi, P., Cocherie, A., Fanning, C.M., Ternet, Y., 2003. Datation U–Pb sur zircons des dolérites tholéiitiques pyrénéennes (ophites) à la limite Trias-Jurassique et relations avec les tufs volcaniques dits «infra-liasiques» nord-pyrénéens. Comptes Rendus des Geosciences 335, 1071–1080.

Sahabi, M., Aslanian, D., Olivet, J.L., 2004. A new starting point for the history of the Central Atlantic. Comptes Rendus des Geosciences 336, 1041–1052.

Sebai, A., Feraud, G., Bertrand, H., Hanes, J., 1991. $^{40}Ar/^{39}Ar$ dating and geochemistry of tholeiitic magmatism related to the early opening of the Central Atlantic Rift. Earth and Planetary Science Letters 104, 455–472.

Schoene B., Crowley, J.L., Condon, D.J., Schmidt, M.D., Bowring, S.A., 2006. Reassessing the uranium decay constants for geochronology using ID-TIMS U–Pb data. Geochimica Cosmochimica Acta 70, 426-445.

Sharp, W.D., Renne, P.R., 2005. The $^{40}Ar/^{39}Ar$ dating of core recovered by the Hawaii Scientific Drilling Project (phase 2), Hilo, Hawaii. *Geochemistry Geophysics Geosystems* **6**, Q04G17.

Schaltegger, U., Schoene, B., Bartolini, A., Guex, J., Ovtcharova, M., 2007. Precise ages for the Triassic/Jurassic boundary and Hettangian recovery from northern Peru. Goldschmidt conference abstract A884, Cologne, Germany.

Simon, J.I., Renne, P.R., Mundil, R., 2008. Implications of pre-eruptive magmatic histories of zircons for U–Pb geochronology of silicic extrusions. Earth and Planetary Science Letters 266, 182-194.

Steiger, R.H., Jäger, E., 1977. Subcommission on geochronology: convention on the use of decay constants in geo- and cosmochronology. Earth and Planetary Science Letters 36, 359–362.

Tanner, L.H., 1996. Formal definition of the Lower Jurassic McCoy Brook Formation, Fundy rift basin, eastern Canada. Atlantic Geology, **32**: 127-136.

Tanner, L.H., 2000. Triassic-Jurassic lacustrine deposition in the Fundy rift basin, Eastern Canada. AAPG Studies in Geology 46, 159-166.

Tanner, L.H., Kyte, F.T., 2005. Anomalous iridium enrichment at the Triassic-Jurassic boundary, Blomidon Formation, Fundy Basin, Canada. Earth and Planetary Science Letters 240, 634-641.

Tanner, L.H., Lucas, S.G., Chapman, M.G., 2004. Assessing the record and causes of late Triassic extinctions. Earth Science Reviews 65, 103–139.

Tanner, L.H., Smith, D.L., Allan, A., 2007. Stomatal response of swordfern to volcanogenic CO_2 and SO_2 from Kilauea volcano, Hawaii. Geophysical Research Letters 34, L15807, doi:10.1029/2007GL030320

Tollo, R.P., and Gottfried, D., 1992, Petrochemistry of Jurassic basalt from eight cores, Newark basin, New Jersey, in Puffer, J.H., and Ragland, P.C., eds., Eastern North American Mesozoic magmatism: Geological Society of America Special Paper 268, p. 233–260.

Tommasi, A., Vauchez, A., 2001. Continental rifting parallel to ancient collisional belts: an effect of the mechanical anisotropy of the lithospheric mantle. Earth and Planetary Science Letters 185, 199– 210.
Van Wijk, J.W., Blackman, D.K., 2005. Dynamics of continental rift propagation: the end-member modes. Earth and Planetary Science Letters 229, 247–258.
Verati, C., Féraud, G., 2003. Ar-Ar plateau ages disturbed by minor alteration phases in plagioclases: How to assess the true duration of brief volcanic events. In: Geophysical Research Abstracts, EGS-AGU-EUG assembly, Nice.
Vérati, C., Bertrand, H., Feraud, G., 2005. The innermost record of CAMP in West Africa: precise $^{40}Ar/^{39}Ar$ dating and geochemistry of Taoudenni basin intrusives (northern Mali). Earth and Planetary Science Letters 235, 391–407.
Vérati, C., Rapaille, C., Féraud, G., Marzoli, A., Bertrand, H., Youbi, N., 2007. Timing the Tr–J boundary: further constraints on duration and age of the CAMP volcanism recorded in Morocco and Portugal. Palaeogeography Palaeoclimatology Palaeoecology 246, doi:10.1016/j.palaeo.2006.06.033.
Villa, I.M., Renne, P.R., 2005. Decay constants in geochronology. Episodes 28, 50-51.
Wilson, M., 1997. Thermal evolution of the Central Atlantic passive margins: continental break-up above a Mesozoic super-plume. Journal of the Geological Society of London 154, 491–495.
Whiteside, J.H., Olsen, P.E., Kent, D.V., Fowell, S.J., Et-Touhami, M., 2007. Synchrony between the Central Atlantic magmatic province and the Triassic–Jurassic mass-extinction event? Palaeogeography, Palaeoclimatology, Palaeoecology 244, 345-367.
White, R., McKenzie, D., 1989. Magmatism at rift zones: the generation of volcanic continental margins and flood basalts. Journal of Geophysical Research 94, 7685– 7729.
Withjack, M.O., Schlische, R.W., Olsen, P.E., 1998. Diachronous rifting, drifting, and inversion on the passive margin of central eastern North America: an analog for other passive margins. AAPG Bulletin 82, 817–835.

Figure and table captions

Figure 1. Sketch map of the remnants of CAMP lava flows, sills and related dykes (modified after McHone (2000) and Knight et al. (2004). SDR: Seaward dipping reflector. Dashed curve indicates the currently known extension of CAMP.

Figure 2. Simplified geological map of the Hartford and Deerfield (U.S.A.) and Fundy (Canada) basins. Ten $^{40}Ar/^{39}Ar$ plateau and one isochron ages (*) are reported in bold. One statistically valid mini-plateau ages is indicated in normal font. Errors are reported at 2σ. Number in italic is a mini-plateau age but with age spectrum showing strong Ar loss, thus discarded in the mean age calculation of the pegmatite lenses.

Figure 3. Synthetic stratigraphic section of the Hartford, Deerfield and Fundy basin sequences. $^{40}Ar/^{39}Ar$ ages obtained on the magmatic units are shown in the sequence. White, black and light gray layers represent sediment, basalt and sill respectively. Pegmatite lenses are indicated in dark gray. * indicates isochron age. Question marks besides light gray indicate that the contacts between sills and lava flows have not been observed in the field. Modified after Whiteside et al. (2007).

Figure 4. $^{40}Ar/^{39}Ar$ apparent age and related Ca/K ratio spectra of the plagioclase separates versus the cumulative percentage of ^{39}Ar released. Errors on plateau (>70% ^{39}Ar released) and mini-plateau ages (50-70%) are quoted at 2σ and do not include systematic errors (i.e.

uncertainties on the age of the monitor and on the decay constant). MSWD and probability (P) are indicated (Ludwig, 2003). Integrated ages are reported (2σ).

Figure 5. Age probability density distribution diagram (PDD) and frequency histogram (error bars not included) of 69 $^{40}Ar/^{39}Ar$ ages of CAMP obtained on plagioclase separates. Age data are from this study and those reported in the compilation by Nomade et al. (2007; and references therein). The PDD curve suggests a total duration of 8-10 Ma for the entire magmatic activity, expressed notably by 2 distinct peaks of activity (see text for interpretation). Both peaks suggest a duration of ~3 Ma.

Figure 6. Weighted mean of CAMP ages by location vs. relative paleolattitude (cf. Fig. 1). Errors are reported at 2σ and are expended by student's t times MSWD to account for the scatter of the data. The weighted means included only ages from the first peak of activity (i.e. >195 Ma). Dashed curve: second order polynomial regression to illustrate the apparent age progression (roughly) from North to South that suggests a migration of the magmatic activity.

Table 1. Summary table indicating integrated, plateau/mini-plateau and isochron ages for the Hartford, Deerfield and Fundy CAMP plagioclase separates. Pl= plateau and MPl = mini plateau. Data in bold are ages that should be added to the filtered compilation by Nomade et al. (2007). MSWD for plateau and mini-plateau and isochron, probability (P) for plateau and mini-plateau, percentage of ^{39}Ar degassed used in the plateau calculation, number of analyses included in the isochron, and $^{40}Ar/^{36}Ar$ intercept are indicated. Analytical uncertainties on the ages are quoted at 2 sigma (2σ) confidence levels and at 1σ for the $^{40}Ar/^{36}Ar$ intercept.

Annex 1. Petrographic picture of HB1 thin section taken in Polarized light. Note the strong sericitization of the plagioclase grains.

Annex 2. Ar data summary table for individual aliquots of Hartford, Deerfield and Fundy CAMP plagioclase separates. Relative Argon abundances are given in nanoamperes (nA) of amplified beam current. Values are corrected for mass discrimination, blanks, and radioactive decay. Errors in parentheses (1σ) are for the smallest significant digits when not otherwise mentioned. $^{40}Ar^*$ = radiogenic argon. Age is based on comparison with the Fish Canyon sanidine monitor (28.03 Ma; Jourdan and Renne, 2007) and on the decay constant of Steiger and Jäger (1977). The J- and discriminations values are indicated for each sample. Laser beam power (W) is provided for each temperature step.

Annex 3. Major (wt.%, electron microprobe, EMP data) compositions of representative sericitized plagioclase crystals of HB1 samples. Note the high K_20 values obtained. For comparison, typical K_20 content of pure CAMP plagioclase is expected to be ~0.1 wt%.

Annex 4. Inverse correlation isochron plot of $^{36}Ar/^{40}Ar$ vs. $^{39}Ar/^{40}Ar$ of sample NS21. Isochron age is given at 2σ and associated error is expended by student's t times MSWD . MSWD and probability are indicated (Ludwig, 2003).

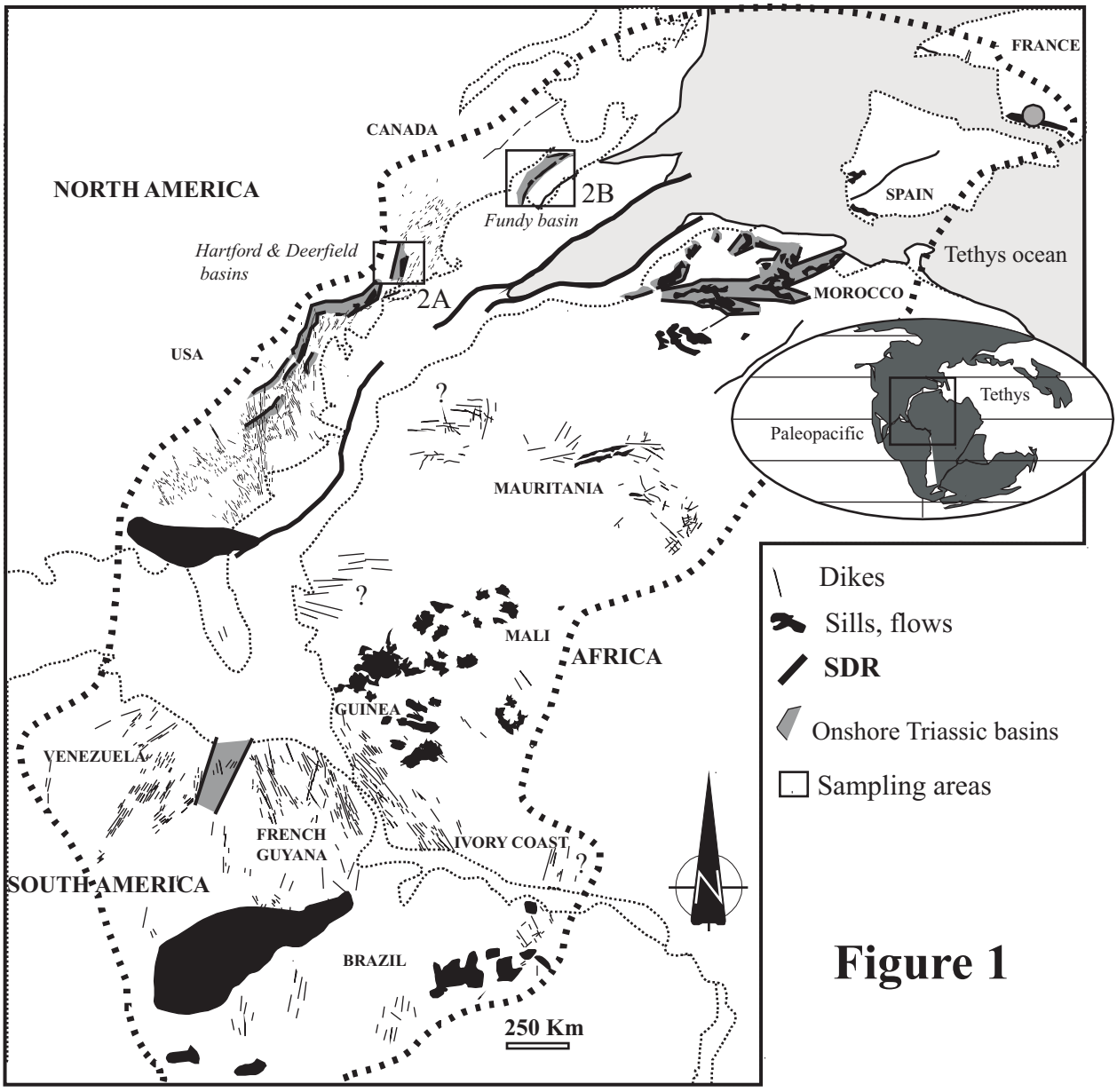
FRANCE
CANADA
NORTH AMERICA
2B
Fundy basin
SPAIN
Hartford & Deerfield
basins
Tethys ocean
2A
MOROCCO
USA
Tethys
Paleopacific
?
MAURITANIA
?
MALI
AFRICA
GUINEA
VENEZUELA
FRENCH
GUYANA
IVORY COAST
?
SOUTH AMERICA
BRAZIL
250 Km
Dikes
Sills, flows
SDR
Onshore Triassic basins
Sampling areas

Figure 1

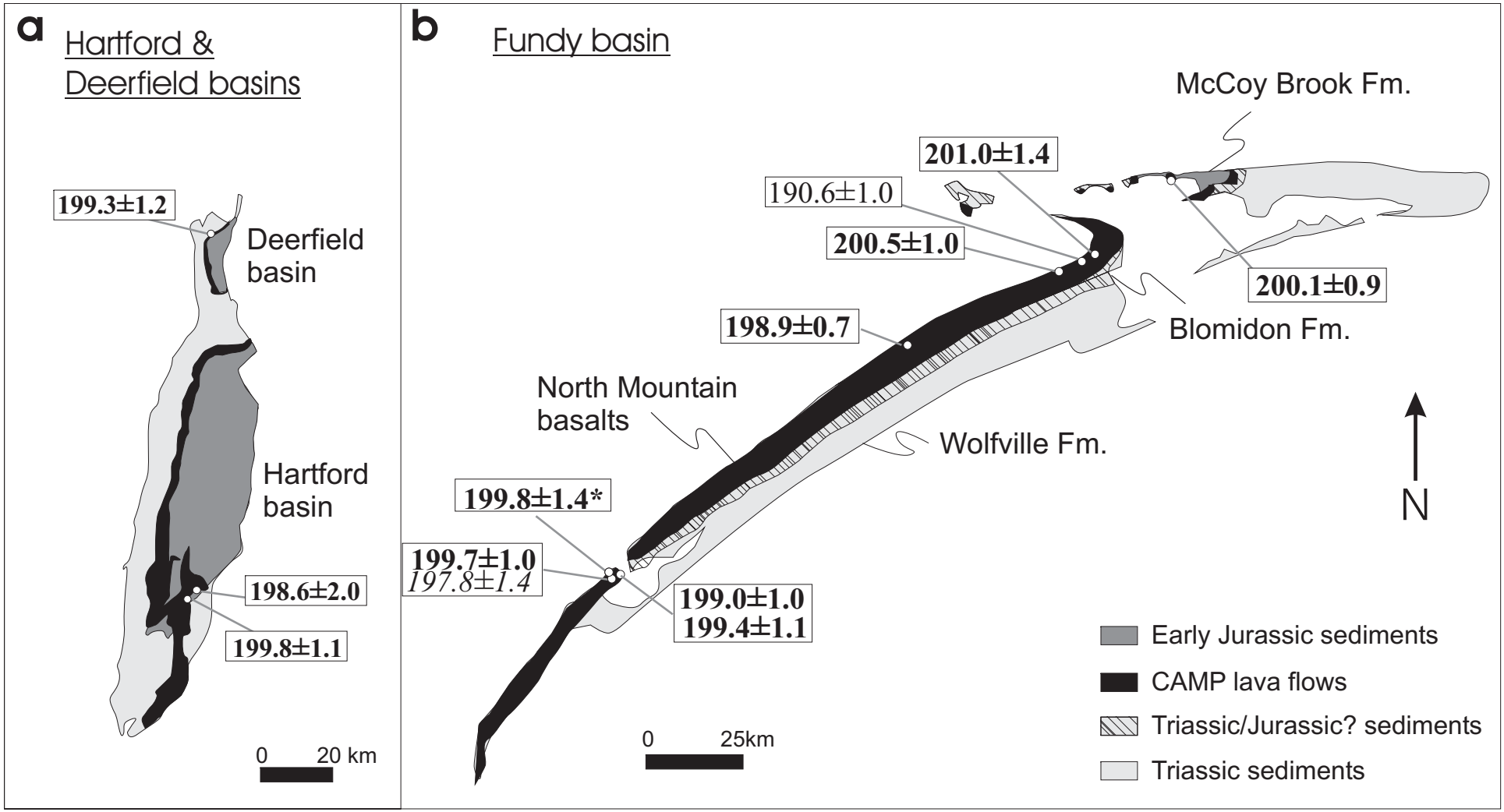

Fig. 2: Jourdan et al.

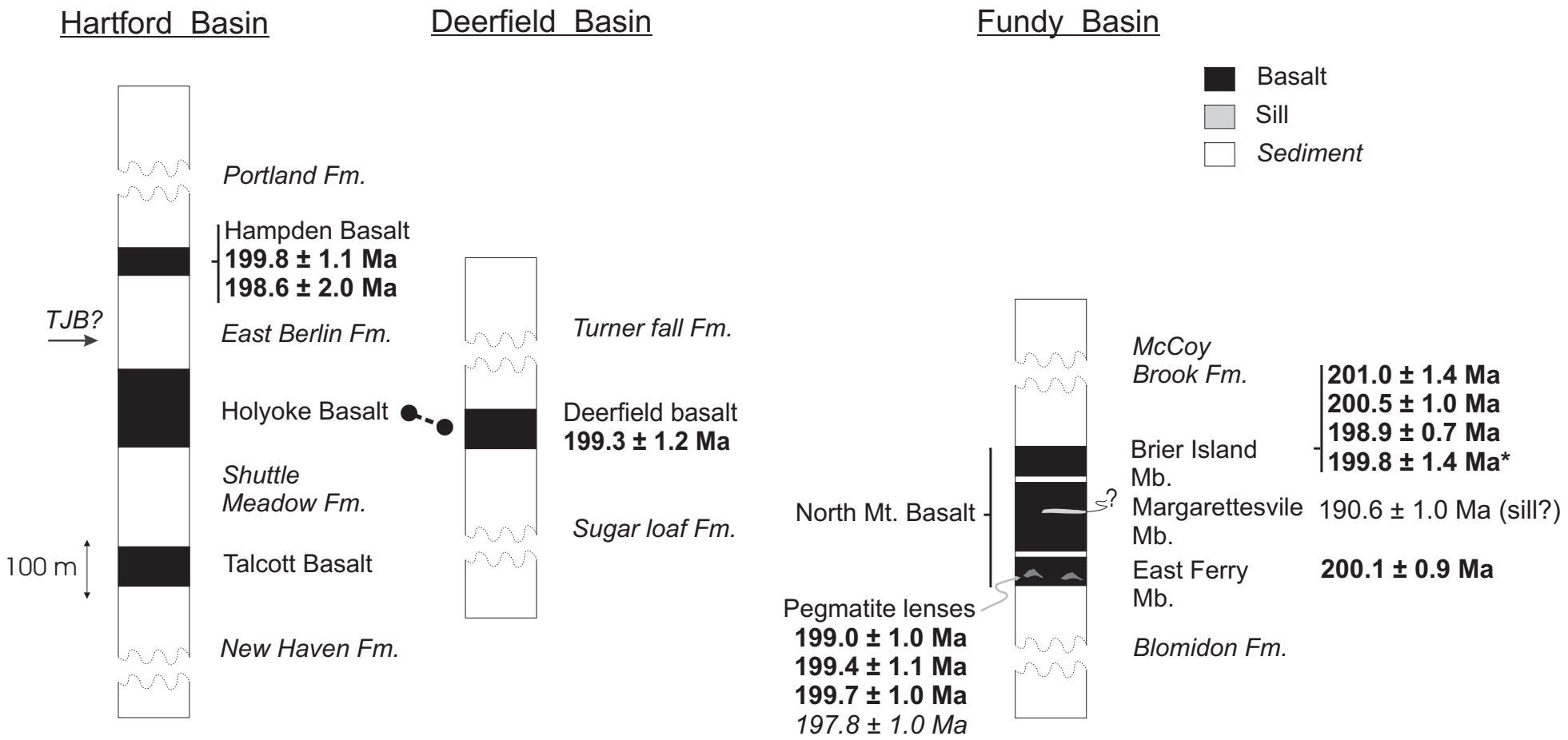

Figure 3: Jourdan et al.

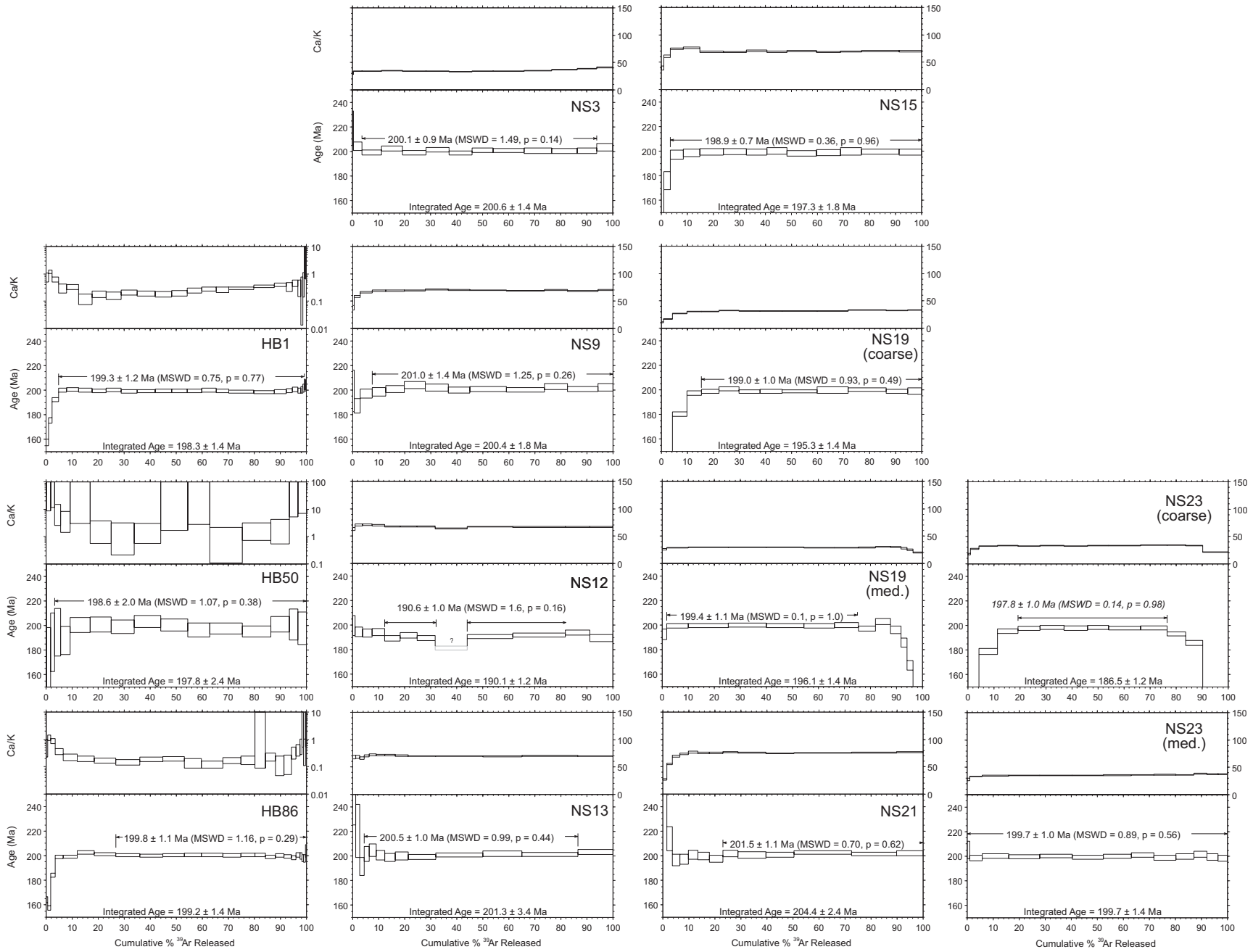

Figure 4: Jourdan et al.

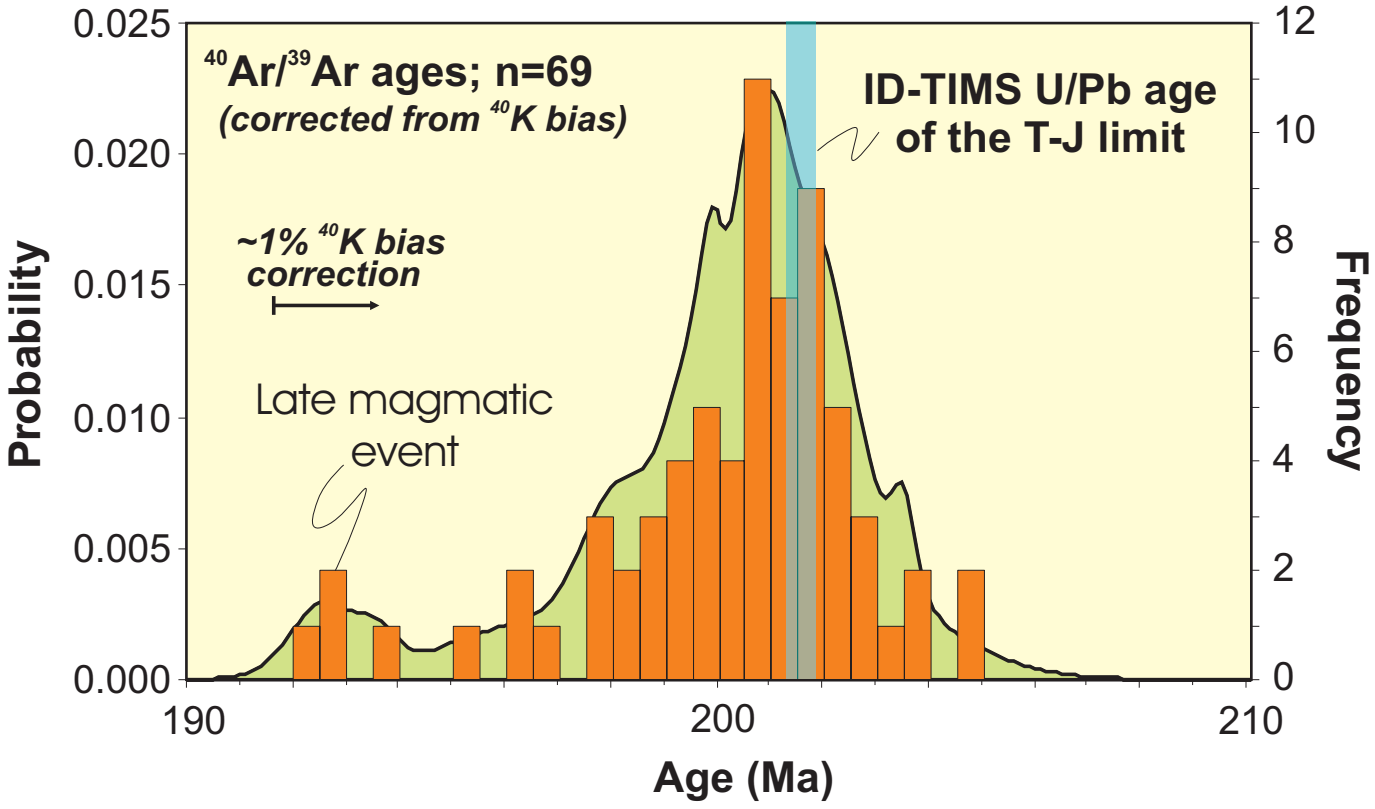

Figure 5: Jourdan et al.

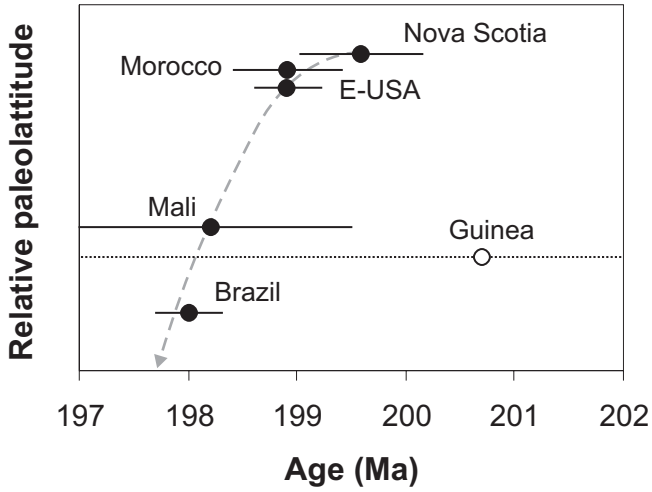

Fig. 6: Jourdan et al.

General characteristics						Plateau characteristics					Isochron characteristics				
Sample N°	Lab N°	Coordinates	Unit	mineral	Integrated age (Ma, ±2σ)	Plateau age (Ma, ±2σ)	Total ^{39}Ar released (%)	Attribute	MSWD	P	Isochron age (Ma, ±2σ)	n	^{40}Ar/^{36}Ar intercept (±1σ)	MSWD	P
Deerfield basin															
HB1	58273-01	42°36'51''N 72°33'06''E	Deerfield (Talcott equi.)	Sericite	198.3 ± 1.4	**199.3 ± 1.2**	94%	Pl	0.75	0.77	205.9 ± 1.2	14	64 ± 6	1.4	0.16
Hartford basin															
HB50	58274-01	41°39'02''N 72°40'04''E	Hampden (upper unit)	Sericite	197.8 ± 2.4	**198.6 ± 2.0**	97%	Pl	1.07	0.38	200.9 ± 2.8	16	256 ± 17	0.86	0.6
HB86	58275-01	41°37'26''N 72°44'14''E	Hampden (upper unit)	Sericite	199.2 ± 1.4	**199.8 ± 1.1**	73%	Pl	1.16	0.29	200.1 ± 1.0	21	266 ± 15	1.4	0.13
Fundy basin															
NS3	58265-01	45°23'43''N 64°11'50''E	East Ferry Member	Plg	200.6 ± 1.4	**200.1 ± 0.9**	90%	Pl	1.50	0.14	199.9 ± 1.2	11	307 ± 10	1.7	0.09
NS9	58252-01	45°18'52''N 64°25'33''E	Brier Island Member	Plg	200.4 ± 1.8	**201.0 ± 1.4**	92%	Pl	1.25	0.26	199.7 ± 2.2	12	330 ± 20	1.3	0.21
NS12	58263-01	45°14'44''N 64°27'23''E	Margaretsville Member (sill?)	Plg	190.1 ± 1.2	190.6 ± 1.0	65%	MPl	1.60	0.16	192.8 ± 1.6	8	282 ± 13	1.9	0.08
NS13	58262-01	45°13'52''N 64°30'50''E	Brier Island Member	Plg	201.3 ± 3.4	**200.5 ± 1.0**	82%	Pl	0.99	0.44	200.6 ± 1.0	12	302 ± 6	1.2	0.28
NS15	58248-01	45°06'14''N 64°56'57''E	Brier Island Member	Plg	197.3 ± 1.8	**198.9 ± 0.7**	97%	Pl	0.36	0.96	199.9 ± 1.4	13	235 ± 7	1.3	0.2
NS19 (coarse)	58287-01	44°39'45''N 65°45'58''E	East Ferry Member (pegmatite lense)	Plg	195.3 ± 1.4	**199.0 ± 1.0**	85%	Pl	0.93	0.49	198.8 ± 1.0	10	297 ± 5	1.4	0.2
NS19 (med.)	58288-01			Plg	196.1 ± 1.4	**199.4 ± 1.1**	74%	Pl	0.07	1	-	-	-	-	-
NS21	58286-01	44°39'55''N 65°49'57''E	Brier Island Member	Plg	204.4 ± 2.4	201.5 ± 1.1	77%	Pl	0.70	0.62	**199.8 ± 1.4**	11	314 ± 4	1.9	0.05
NS23 (coarse)	58290-01	44°39'09''N 65°47'50''E	East Ferry Member (pegmatite lense)	Plg	186.5 ± 1.2	197.8 ± 1.0	57%	MPl	0.14	0.98	-	-	-	-	-
NS23 (med.)	58289-01			Plg	199.7 ± 1.4	**199.7 ± 1.0**	100%	Pl	0.89	0.56	199.6 ± 1.0	13	310 ± 40	0.95	0.49

Table 2: Jourdan et al.

Sample N°	Laser intensity (W)	^{40}Ar ±σ (nA)	^{39}Ar ±σ (nA)	^{38}Ar ±σ (nA)	^{37}Ar ±σ (nA)	^{36}Ar ±σ (nA)	^{40}Ar* ±σ (%)	^{40}Ar*/^{39}Ar$_K$ ±σ	Age ±σ
HB1		*JDisc1 = 0.002672 ± 0.000008 (0.28%)*			*D=1.00654 ± 0.00248*				
58273-01A	1.0	0.1162 (25)	0.00205 (7)	0.000064 (22)	-0.0064 (37)	0.000138 (21)	64.4 ± 6.0	36.5 ± 3.6	167.5 ± 15.8
58273-01B	2.0	2.6731 (44)	0.05579 (21)	0.001422 (31)	0.0219 (39)	0.002599 (26)	71.3 ± 0.3	34.2 ± 0.3	157.5 ± 1.3
58273-01C	2.5	4.2267 (48)	0.08860 (30)	0.001933 (38)	0.0533 (41)	0.002856 (26)	80.1 ± 0.2	38.2 ± 0.3	175.3 ± 1.1
58273-01D	3.0	6.7115 (60)	0.14249 (33)	0.002496 (41)	0.0454 (45)	0.002421 (26)	89.4 ± 0.2	42.1 ± 0.2	192.1 ± 0.8
58273-01E	3.5	8.5693 (61)	0.18250 (41)	0.002602 (63)	0.0285 (53)	0.001896 (28)	93.5 ± 0.1	43.9 ± 0.2	199.8 ± 0.8
58273-01F	4.0	12.4771 (72)	0.26825 (57)	0.003796 (54)	0.0448 (45)	0.002280 (28)	94.6 ± 0.1	44.0 ± 0.2	200.3 ± 0.7
58273-01G	4.4	13.9468 (90)	0.30451 (77)	0.004068 (50)	0.0197 (43)	0.001961 (28)	95.9 ± 0.1	43.9 ± 0.2	199.8 ± 0.8
58273-01H	4.8	14.5528 (76)	0.32000 (81)	0.004362 (54)	0.0294 (41)	0.001858 (26)	96.2 ± 0.1	43.8 ± 0.2	199.3 ± 0.7
58273-01I	5.2	15.8219 (93)	0.34459 (66)	0.004722 (60)	0.0281 (44)	0.002295 (27)	95.7 ± 0.1	44.0 ± 0.2	200.0 ± 0.7
58273-01J	5.5	16.5663 (88)	0.36360 (73)	0.004977 (64)	0.0386 (40)	0.002370 (27)	95.8 ± 0.1	43.6 ± 0.2	198.7 ± 0.7
58273-01K	6.0	18.4568 (97)	0.40511 (74)	0.005609 (47)	0.0395 (41)	0.002566 (28)	95.9 ± 0.1	43.7 ± 0.2	198.9 ± 0.7
58273-01L	6.3	16.8938 (88)	0.37114 (77)	0.005165 (60)	0.0339 (39)	0.002262 (28)	96.1 ± 0.1	43.7 ± 0.2	199.1 ± 0.7
58273-01M	6.7	16.2703 (91)	0.35605 (75)	0.005016 (49)	0.0355 (41)	0.002344 (27)	95.8 ± 0.1	43.8 ± 0.2	199.2 ± 0.7
58273-01N	7.0	15.1508 (91)	0.32980 (83)	0.004665 (60)	0.0412 (42)	0.002426 (27)	95.3 ± 0.1	43.8 ± 0.2	199.3 ± 0.8
58273-01O	7.5	14.9181 (79)	0.32405 (79)	0.004605 (54)	0.0461 (41)	0.002377 (28)	95.3 ± 0.1	43.9 ± 0.2	199.7 ± 0.7
58273-01P	7.8	13.0601 (77)	0.28403 (62)	0.004206 (60)	0.0378 (41)	0.002172 (28)	95.1 ± 0.1	43.7 ± 0.2	199.1 ± 0.7
58273-01Q	8.9	26.1647 (132)	0.57214 (94)	0.008243 (60)	0.0844 (44)	0.004171 (33)	95.3 ± 0.1	43.6 ± 0.2	198.5 ± 0.7
58273-01R	10	20.9972 (123)	0.45841 (89)	0.006668 (64)	0.0800 (42)	0.003579 (31)	95.0 ± 0.1	43.5 ± 0.2	198.2 ± 0.7
58273-01S	11.5	12.9018 (71)	0.27785 (66)	0.004301 (56)	0.0562 (39)	0.002664 (27)	93.9 ± 0.1	43.6 ± 0.2	198.6 ± 0.8
58273-01T	13	5.9089 (56)	0.12645 (31)	0.002060 (44)	0.0227 (41)	0.001275 (24)	93.7 ± 0.2	43.8 ± 0.2	199.3 ± 0.8
58273-01U	16.5	6.1858 (58)	0.12829 (38)	0.002181 (42)	0.0299 (40)	0.001827 (25)	91.3 ± 0.2	44.0 ± 0.2	200.4 ± 0.9
58273-01V	20	3.4714 (45)	0.07297 (24)	0.001231 (31)	0.0133 (40)	0.000931 (24)	92.1 ± 0.3	43.8 ± 0.2	199.5 ± 1.0
58273-01W	23	1.9275 (31)	0.04047 (17)	0.000720 (31)	0.0077 (38)	0.000507 (22)	92.3 ± 0.4	43.9 ± 0.3	200.0 ± 1.3
58273-01X	26	1.5793 (30)	0.03262 (19)	0.000530 (27)	0.0101 (40)	0.000462 (22)	91.4 ± 0.5	44.3 ± 0.4	201.4 ± 1.6
58273-01Y	31	1.1425 (29)	0.02303 (17)	0.000405 (29)	-0.0002 (41)	0.000362 (22)	90.6 ± 0.7	45.0 ± 0.5	204.4 ± 2.1
58273-01Z	35	0.9641 (29)	0.01984 (14)	0.000302 (25)	-0.0011 (38)	0.000257 (22)	92.1 ± 0.8	44.7 ± 0.5	203.5 ± 2.2
HB50		*JDisc3 = 0.002668 ± 0.000007 (0.25%)*			*D=1.00654 ± 0.00248*				
58274-01A	1.0	0.0116 (18)	0.00033 (12)	0.000008 (23)	-0.0051 (51)	-0.000007 (15)	114.3 ± 46.0	39.4 ± 20.7	180.5 ± 90.3
58274-01B	2.0	0.1546 (18)	0.00240 (13)	0.000103 (26)	0.0002 (51)	0.000218 (16)	58.4 ± 3.4	37.6 ± 3.0	172.4 ± 12.9
58274-01C	2.5	0.2070 (19)	0.00271 (12)	0.000122 (25)	0.0056 (50)	0.000328 (16)	53.4 ± 2.6	40.8 ± 2.7	186.3 ± 11.9
58274-01D	3.0	0.2206 (18)	0.00347 (13)	0.000144 (25)	0.0151 (54)	0.000253 (16)	66.7 ± 2.4	42.6 ± 2.2	194.2 ± 9.7
58274-01E	3.5	0.3001 (18)	0.00586 (14)	0.000152 (24)	0.0143 (51)	0.000207 (16)	80.0 ± 1.8	41.0 ± 1.3	187.5 ± 5.7
58274-01F	4.4	0.5817 (22)	0.01206 (14)	0.000214 (26)	0.0082 (51)	0.000176 (16)	91.2 ± 1.0	44.0 ± 0.7	200.2 ± 3.0
58274-01G	4.9	0.6125 (23)	0.01273 (16)	0.000232 (27)	0.0137 (51)	0.000179 (16)	91.6 ± 0.9	44.1 ± 0.7	200.7 ± 3.0
58274-01H	5.5	0.6635 (23)	0.01406 (16)	0.000206 (25)	0.0118 (52)	0.000171 (16)	92.5 ± 0.9	43.7 ± 0.6	198.9 ± 2.7
58274-01I	6.3	0.7754 (25)	0.01633 (16)	0.000244 (25)	0.0146 (51)	0.000161 (16)	94.0 ± 0.7	44.7 ± 0.6	203.1 ± 2.5
58274-01J	7.0	0.7649 (23)	0.01635 (16)	0.000224 (26)	0.0034 (51)	0.000154 (16)	94.1 ± 0.7	44.0 ± 0.6	200.3 ± 2.4
58274-01K	7.8	0.6193 (23)	0.01339 (16)	0.000218 (24)	0.0081 (53)	0.000150 (16)	93.0 ± 0.9	43.0 ± 0.7	196.1 ± 2.8
58274-01L	10	0.9128 (26)	0.01967 (18)	0.000300 (26)	0.0113 (52)	0.000209 (16)	93.3 ± 0.7	43.3 ± 0.5	197.3 ± 2.2
58274-01M	13	0.8096 (26)	0.01745 (16)	0.000257 (25)	0.0167 (52)	0.000220 (16)	92.1 ± 0.7	42.8 ± 0.5	195.0 ± 2.3
58274-01O	20	0.5297 (20)	0.01106 (14)	0.000180 (25)	0.0131 (51)	0.000148 (16)	92.0 ± 1.0	44.1 ± 0.7	200.7 ± 3.2
58274-01P	26	0.2612 (19)	0.00528 (13)	0.000110 (24)	0.0033 (52)	0.000096 (16)	89.2 ± 2.0	44.1 ± 1.5	200.7 ± 6.3
58274-01Q	35	0.2428 (18)	0.00499 (13)	0.000100 (24)	0.0074 (52)	0.000092 (15)	89.1 ± 2.1	43.4 ± 1.5	197.5 ± 6.6
HB86		*JDisc3 = 0.002668 ± 0.000007 (0.25%)*			*D=1.00654 ± 0.00248*				
58275-01A	1.0	0.0328 (5)	0.00057 (5)	0.000032 (14)	0.0128 (25)	0.000063 (9)	46.5 ± 8.6	27.1 ± 5.6	125.8 ± 25.2
58275-01B	2.0	1.1177 (14)	0.02751 (15)	0.000478 (21)	0.0082 (26)	0.000466 (11)	87.8 ± 0.3	35.7 ± 0.3	163.9 ± 1.2
58275-01C	2.5	1.5253 (17)	0.04131 (18)	0.000669 (23)	0.0241 (28)	0.000398 (11)	92.4 ± 0.3	34.1 ± 0.2	157.3 ± 0.9
58275-01D	3.0	2.8307 (31)	0.06748 (24)	0.000928 (26)	0.0301 (30)	0.000404 (11)	95.9 ± 0.2	40.2 ± 0.2	183.9 ± 0.9
58275-01E	3.5	5.3525 (45)	0.11990 (28)	0.001531 (38)	0.0223 (29)	0.000392 (12)	97.9 ± 0.1	43.7 ± 0.2	198.9 ± 0.7
58275-01F	4.0	8.9779 (55)	0.20194 (37)	0.002583 (44)	0.0230 (30)	0.000496 (13)	98.4 ± 0.1	43.7 ± 0.1	199.1 ± 0.6
58275-01G	4.4	11.2672 (65)	0.25052 (70)	0.003165 (43)	0.0245 (28)	0.000387 (13)	99.0 ± 0.1	44.5 ± 0.2	202.5 ± 0.7
58275-01H	4.8	14.3535 (71)	0.32177 (75)	0.004131 (45)	0.0277 (28)	0.000478 (15)	99.0 ± 0.1	44.2 ± 0.2	201.0 ± 0.7
58275-01I	5.2	15.6881 (91)	0.35304 (74)	0.004503 (56)	0.0265 (32)	0.000531 (15)	99.0 ± 0.1	44.0 ± 0.2	200.2 ± 0.6
58275-01J	5.5	14.9556 (80)	0.33790 (69)	0.004263 (50)	0.0327 (31)	0.000461 (13)	99.1 ± 0.1	43.9 ± 0.1	199.7 ± 0.6
58275-01K	6.0	14.2448 (74)	0.32087 (61)	0.004142 (59)	0.0324 (31)	0.000435 (14)	99.1 ± 0.1	44.0 ± 0.1	200.3 ± 0.6
58275-01L	6.3	11.0145 (76)	0.24775 (65)	0.003122 (38)	0.0181 (36)	0.000339 (14)	99.1 ± 0.1	44.1 ± 0.2	200.5 ± 0.7
58275-01M	6.7	14.0710 (70)	0.31700 (78)	0.003928 (56)	0.0199 (30)	0.000375 (14)	99.2 ± 0.1	44.0 ± 0.2	200.4 ± 0.7
58275-01N	7.0	11.8585 (70)	0.26757 (58)	0.003260 (43)	0.0234 (29)	0.000353 (14)	99.1 ± 0.1	43.9 ± 0.2	200.0 ± 0.7
58275-01O	7.5	9.0937 (54)	0.20472 (44)	0.002608 (47)	0.0184 (31)	0.000272 (12)	99.1 ± 0.1	44.0 ± 0.2	200.4 ± 0.7
58275-01P	7.8	6.8199 (58)	0.15377 (36)	0.002007 (36)	0.0012 (29)	0.000161 (12)	99.3 ± 0.1	44.0 ± 0.2	200.4 ± 0.7
58275-01Q	8.9	6.6403 (58)	0.15079 (28)	0.001937 (38)	0.0178 (29)	0.000194 (13)	99.2 ± 0.1	43.7 ± 0.1	198.8 ± 0.6
58275-01R	10	5.4743 (45)	0.12334 (32)	0.001648 (46)	0.0089 (30)	0.000190 (12)	99.0 ± 0.1	43.9 ± 0.2	200.0 ± 0.7
58275-01S	11.5	4.9041 (47)	0.11057 (30)	0.001409 (35)	0.0087 (29)	0.000236 (13)	98.6 ± 0.2	43.7 ± 0.2	199.1 ± 0.8
58275-01T	13	2.9742 (38)	0.06664 (21)	0.000932 (29)	0.0118 (27)	0.000253 (11)	97.5 ± 0.2	43.5 ± 0.2	198.2 ± 0.9
58275-01U	16.5	2.7487 (36)	0.05937 (21)	0.000890 (25)	0.0130 (30)	0.000461 (13)	95.1 ± 0.2	44.0 ± 0.2	200.4 ± 1.0
58275-01V	20	1.5473 (16)	0.03181 (15)	0.000507 (23)	0.0104 (31)	0.000524 (14)	90.1 ± 0.3	43.8 ± 0.3	199.5 ± 1.3
58275-01W	23	1.1500 (19)	0.02440 (13)	0.000340 (25)	0.0012 (26)	0.000310 (12)	92.0 ± 0.4	43.4 ± 0.3	197.6 ± 1.4
58275-01X	30	1.2083 (16)	0.02533 (16)	0.000388 (22)	0.0072 (30)	0.000374 (12)	90.9 ± 0.3	43.4 ± 0.4	197.5 ± 1.5
58275-01Y	35	0.5710 (13)	0.01227 (13)	0.000155 (19)	-0.0027 (30)	0.000072 (10)	96.2 ± 0.6	44.8 ± 0.6	203.6 ± 2.5
NS3		*JDisc2 = 0.002675 ± 0.000004 (0.15%)*			*D=1.00646 ± 0.00238*				
58265-01A	2.0	0.2771 (32)	0.00477 (9)	0.000125 (19)	0.0749 (34)	0.000189 (18)	82.0 ± 2.5	48.2 ± 1.6	218.7 ± 7.0
58265-01B	3.0	1.2336 (36)	0.02728 (18)	0.000372 (23)	0.4697 (46)	0.000221 (19)	97.7 ± 0.6	44.8 ± 0.4	204.1 ± 1.8
58265-01C	4.0	2.8782 (54)	0.06621 (24)	0.000877 (30)	1.1557 (66)	0.000411 (20)	99.0 ± 0.3	43.6 ± 0.2	199.1 ± 1.0
58265-01D	4.8	3.0718 (54)	0.06996 (26)	0.000921 (29)	1.2375 (86)	0.000376 (19)	99.6 ± 0.3	44.3 ± 0.2	202.2 ± 1.0
58265-01E	5.5	3.3908 (52)	0.07842 (26)	0.001045 (29)	1.3720 (77)	0.000453 (20)	99.3 ± 0.3	43.5 ± 0.2	198.6 ± 0.9
58265-01F	6.3	3.3664 (54)	0.07695 (27)	0.000959 (32)	1.3385 (74)	0.000427 (19)	99.4 ± 0.3	44.1 ± 0.2	201.1 ± 0.9
58265-01G	7.0	3.3089 (47)	0.07641 (23)	0.001036 (29)	1.2829 (94)	0.000444 (19)	99.1 ± 0.3	43.5 ± 0.2	198.5 ± 0.9
58265-01H	7.8	3.0960 (51)	0.07070 (23)	0.000901 (27)	1.2250 (83)	0.000425 (20)	99.1 ± 0.3	44.0 ± 0.2	200.7 ± 0.9
58265-01I	10	4.5622 (59)	0.10311 (31)	0.001373 (31)	1.7969 (93)	0.000781 (20)	98.1 ± 0.2	44.0 ± 0.2	200.7 ± 0.8
58265-01J	13	4.6578 (56)	0.09172 (25)	0.001588 (31)	1.6275 (83)	0.002753 (25)	85.3 ± 0.2	43.9 ± 0.2	200.4 ± 1.0
58265-01K	20	3.8899 (68)	0.08425 (28)	0.001299 (29)	1.5544 (75)	0.001257 (21)	93.6 ± 0.3	43.9 ± 0.2	200.1 ± 1.0

58265-01L	26	3.1657 (60)	0.06661 (24)	0.001031 (27)	1.3160 (85)	0.001325 (21)	91.0 ± 0.3	43.9 ± 0.3	200.3 ± 1.1
58265-01M	35	2.7715 (56)	0.05213 (24)	0.000929 (29)	1.0806 (74)	0.001928 (23)	82.6 ± 0.4	44.6 ± 0.3	203.3 ± 1.4
NS9		*JDisc1 = 0.002672 ± 0.000008 (0.28%)*			*D=1.00646 ± 0.00238*				
58252-01A	2.0	0.2212 (32)	0.00386 (8)	0.000103 (19)	0.0743 (37)	0.000206 (18)	75.2 ± 3.0	43.7 ± 1.9	199.2 ± 8.4
58252-01B	3.0	0.5387 (33)	0.01266 (13)	0.000185 (21)	0.3739 (51)	0.000212 (18)	93.9 ± 1.3	40.9 ± 0.7	187.0 ± 2.9
58252-01C	4.0	1.0942 (46)	0.02514 (15)	0.000347 (22)	0.8420 (72)	0.000353 (19)	96.6 ± 0.8	43.1 ± 0.4	196.8 ± 1.8
58252-01D	4.8	1.2728 (44)	0.02921 (19)	0.000402 (23)	1.0253 (83)	0.000399 (19)	97.2 ± 0.7	43.5 ± 0.4	198.4 ± 1.8
58252-01E	5.5	1.6993 (51)	0.03843 (18)	0.000542 (25)	1.3410 (116)	0.000544 (20)	96.8 ± 0.5	44.0 ± 0.3	200.5 ± 1.4
58252-01F	6.3	2.1575 (58)	0.04536 (20)	0.000654 (25)	1.5999 (92)	0.001049 (21)	91.5 ± 0.5	44.7 ± 0.3	203.8 ± 1.4
58252-01G	7.0	2.3434 (60)	0.04864 (22)	0.000745 (27)	1.7496 (90)	0.001311 (22)	89.4 ± 0.4	44.3 ± 0.3	201.8 ± 1.4
58252-01H	7.8	2.0218 (42)	0.04531 (20)	0.000643 (24)	1.6220 (84)	0.000741 (20)	95.6 ± 0.4	43.8 ± 0.3	199.9 ± 1.3
58252-01I	10	3.5776 (55)	0.07800 (28)	0.001148 (32)	2.7689 (106)	0.001546 (21)	93.4 ± 0.3	44.0 ± 0.2	200.7 ± 1.0
58252-01J	13	3.5941 (54)	0.08011 (27)	0.001089 (32)	2.8080 (126)	0.001345 (21)	95.2 ± 0.3	43.9 ± 0.2	200.0 ± 1.0
58252-01K	20	2.1912 (42)	0.04887 (21)	0.000650 (26)	1.7479 (96)	0.000726 (20)	96.6 ± 0.4	44.5 ± 0.3	202.7 ± 1.2
58252-01L	26	2.8424 (47)	0.06424 (23)	0.000867 (28)	2.2343 (107)	0.000907 (20)	96.8 ± 0.3	44.0 ± 0.2	200.6 ± 1.0
58252-01M	35	1.4097 (39)	0.03181 (16)	0.000407 (25)	1.1335 (74)	0.000432 (19)	97.4 ± 0.6	44.3 ± 0.3	202.1 ± 1.5
NS12		*JDisc2 = 0.002675 ± 0.000004 (0.15%)*			*D=1.00646 ± 0.00238*				
58263-01A	2.0	0.0545 (7)	0.00071 (6)	0.000025 (19)	0.0179 (30)	0.000063 (13)	68.4 ± 7.5	53.4 ± 7.3	240.7 ± 30.7
58263-01B	3.0	0.2592 (13)	0.00572 (6)	0.000101 (21)	0.1823 (38)	0.000102 (14)	94.0 ± 1.7	43.7 ± 0.9	199.4 ± 4.0
58263-01C	4.0	0.7120 (13)	0.01655 (12)	0.000235 (21)	0.5907 (48)	0.000253 (14)	96.1 ± 0.6	42.5 ± 0.4	194.2 ± 1.9
58263-01D	4.8	0.8675 (12)	0.02060 (14)	0.000279 (23)	0.7379 (55)	0.000268 (14)	97.7 ± 0.5	42.3 ± 0.4	193.3 ± 1.7
58263-01E	5.5	1.1970 (17)	0.02841 (17)	0.000362 (22)	1.0084 (68)	0.000348 (15)	98.1 ± 0.4	42.5 ± 0.3	194.2 ± 1.4
58263-01F	6.3	1.3680 (17)	0.03350 (16)	0.000459 (23)	1.1537 (62)	0.000380 (15)	98.5 ± 0.4	41.3 ± 0.3	189.1 ± 1.2
58263-01G	7.0	1.5932 (20)	0.03851 (17)	0.000498 (23)	1.3154 (72)	0.000434 (15)	98.5 ± 0.3	41.8 ± 0.3	191.4 ± 1.1
58263-01H	7.8	1.6049 (25)	0.03942 (16)	0.000554 (24)	1.3526 (69)	0.000429 (15)	98.8 ± 0.4	41.3 ± 0.2	189.1 ± 1.1
58263-01I	10	2.7697 (39)	0.07088 (22)	0.000879 (30)	2.2941 (98)	0.000763 (16)	98.5 ± 0.3	39.4 ± 0.2	181.0 ± 0.8
58263-01J	13	4.0939 (39)	0.10030 (25)	0.001243 (31)	3.4234 (106)	0.001019 (17)	99.3 ± 0.2	41.6 ± 0.2	190.4 ± 0.7
58263-01K	20	4.8451 (46)	0.11627 (29)	0.001544 (31)	3.9356 (114)	0.001393 (17)	98.0 ± 0.2	41.9 ± 0.2	191.7 ± 0.7
58263-01L	26	2.4450 (33)	0.05470 (18)	0.000842 (30)	1.8513 (90)	0.001137 (18)	92.3 ± 0.3	42.3 ± 0.2	193.6 ± 1.0
58263-01M	35	2.5963 (36)	0.05030 (21)	0.001039 (26)	1.6999 (82)	0.002386 (20)	78.1 ± 0.3	41.4 ± 0.3	189.3 ± 1.4
NS13		*JDisc2 = 0.002675 ± 0.000004 (0.15%)*			*D=1.00646 ± 0.00238*				
58262-01A	2.0	14.8805 (190)	0.00837 (16)	0.009555 (76)	0.2903 (38)	0.048155 (76)	4.5 ± 0.2	82.7 ± 17.2	360.7 ± 67.9
58262-01B	3.0	2.3656 (61)	0.00939 (11)	0.001397 (30)	0.3273 (46)	0.006594 (31)	18.7 ± 0.5	48.5 ± 2.5	220.1 ± 10.7
58262-01C	4.0	0.6147 (31)	0.01001 (9)	0.000290 (21)	0.3373 (45)	0.000792 (20)	66.3 ± 1.1	41.8 ± 0.8	191.1 ± 3.7
58262-01D	4.8	0.6577 (32)	0.01319 (13)	0.000212 (21)	0.4716 (53)	0.000436 (19)	86.1 ± 1.1	44.1 ± 0.7	201.4 ± 3.0
58262-01E	5.5	0.7745 (32)	0.01625 (13)	0.000269 (22)	0.5968 (61)	0.000385 (19)	91.5 ± 0.9	44.8 ± 0.6	204.4 ± 2.5
58262-01F	6.3	0.9356 (32)	0.02058 (13)	0.000277 (22)	0.7523 (60)	0.000396 (19)	93.9 ± 0.8	43.9 ± 0.5	200.4 ± 2.0
58262-01G	7.0	1.1584 (34)	0.02590 (13)	0.000371 (23)	0.9446 (68)	0.000470 (20)	94.5 ± 0.7	43.5 ± 0.4	198.5 ± 1.6
58262-01H	7.8	1.3501 (34)	0.03039 (19)	0.000378 (24)	1.0896 (71)	0.000481 (19)	95.9 ± 0.6	43.8 ± 0.4	199.9 ± 1.7
58262-01I	10	2.9726 (45)	0.06735 (25)	0.000917 (30)	2.3917 (109)	0.001044 (21)	96.0 ± 0.3	43.6 ± 0.2	198.9 ± 1.0
58262-01J	13	4.9939 (53)	0.11279 (32)	0.001602 (35)	3.9974 (138)	0.001646 (23)	96.6 ± 0.2	44.0 ± 0.2	200.7 ± 0.8
58262-01K	20	4.6463 (60)	0.09441 (28)	0.001543 (32)	3.3253 (119)	0.002878 (26)	87.4 ± 0.2	44.2 ± 0.2	201.6 ± 1.0
58262-01L	26	6.0114 (67)	0.13506 (36)	0.001855 (30)	4.8309 (157)	0.002065 (23)	96.3 ± 0.2	44.0 ± 0.2	200.9 ± 0.8
58262-01M	35	3.8366 (74)	0.08408 (27)	0.001203 (31)	2.9868 (119)	0.001464 (21)	94.9 ± 0.3	44.5 ± 0.2	203.0 ± 1.0
NS15		*JDisc1 = 0.002672 ± 0.000008 (0.28%)*			*D=1.00646 ± 0.00238*				
58248-01A	2.0	0.5753 (26)	0.00418 (16)	0.000852 (47)	0.0830 (28)	0.001662 (21)	15.8 ± 1.2	22.0 ± 2.2	103.2 ± 9.9
58248-01B	3.0	0.5006 (21)	0.01011 (15)	0.000549 (28)	0.3117 (41)	0.000498 (17)	75.6 ± 1.1	38.3 ± 0.8	175.9 ± 3.7
58248-01C	4.0	0.9223 (23)	0.02072 (14)	0.000376 (25)	0.7802 (52)	0.000394 (15)	94.1 ± 0.6	43.1 ± 0.4	196.9 ± 1.8
58248-01D	4.8	1.1276 (17)	0.02581 (16)	0.000399 (23)	1.0012 (67)	0.000402 (15)	96.5 ± 0.4	43.5 ± 0.4	198.3 ± 1.6
58248-01E	5.5	1.6012 (24)	0.03692 (19)	0.000552 (26)	1.2918 (70)	0.000453 (15)	98.1 ± 0.3	43.7 ± 0.3	199.3 ± 1.3
58248-01F	6.3	1.5732 (24)	0.03620 (17)	0.000494 (24)	1.2648 (74)	0.000452 (15)	97.9 ± 0.4	43.7 ± 0.3	199.4 ± 1.2
58248-01G	7.0	1.4271 (23)	0.03247 (16)	0.000467 (24)	1.1678 (64)	0.000480 (15)	96.6 ± 0.4	43.6 ± 0.3	199.0 ± 1.3
58248-01H	7.8	1.3541 (21)	0.03092 (17)	0.000518 (28)	1.0860 (71)	0.000406 (15)	97.5 ± 0.4	43.9 ± 0.3	200.0 ± 1.4
58248-01I	10	2.0267 (30)	0.04643 (20)	0.000763 (28)	1.6596 (80)	0.000674 (16)	96.7 ± 0.3	43.4 ± 0.3	197.9 ± 1.1
58248-01J	13	1.6494 (21)	0.03785 (19)	0.000590 (28)	1.3197 (65)	0.000505 (16)	97.3 ± 0.3	43.6 ± 0.3	198.7 ± 1.3
58248-01K	20	1.4337 (25)	0.03274 (21)	0.000611 (29)	1.1522 (63)	0.000438 (16)	97.4 ± 0.4	43.8 ± 0.4	199.7 ± 1.5
58248-01L	26	2.5273 (36)	0.05852 (24)	0.000870 (29)	2.0946 (86)	0.000699 (17)	98.4 ± 0.3	43.7 ± 0.2	199.3 ± 1.1
58248-01M	35	1.5383 (20)	0.03531 (17)	0.000483 (24)	1.2530 (64)	0.000471 (15)	97.5 ± 0.4	43.6 ± 0.3	199.0 ± 1.3
NS19 (coarse)		*JDisc4 = 0.002664 ± 0.000005 (0.20%)*			*D=1.00646 ± 0.00238*				
58287-01B	3.0	1.5187 (61)	0.04779 (26)	0.000661 (23)	0.4103 (55)	0.000307 (19)	96.2 ± 0.7	30.8 ± 0.3	142.1 ± 1.2
58287-01C	4.0	2.8933 (64)	0.07298 (26)	0.000908 (31)	0.9830 (58)	0.000424 (20)	98.4 ± 0.4	39.4 ± 0.2	180.1 ± 0.9
58287-01D	4.8	3.3343 (61)	0.07701 (24)	0.001013 (29)	1.1746 (75)	0.000434 (19)	99.0 ± 0.3	43.3 ± 0.2	197.2 ± 0.9
58287-01E	5.5	4.0092 (60)	0.09190 (26)	0.001229 (28)	1.4371 (89)	0.000539 (20)	98.9 ± 0.3	43.7 ± 0.2	198.5 ± 0.8
58287-01F	6.3	4.5592 (63)	0.10350 (31)	0.001352 (30)	1.6833 (111)	0.000614 (20)	99.0 ± 0.2	44.1 ± 0.2	200.6 ± 0.8
58287-01G	7.0	4.7861 (54)	0.11003 (29)	0.001453 (31)	1.7430 (82)	0.000627 (20)	99.0 ± 0.2	43.6 ± 0.2	198.3 ± 0.8
58287-01H	7.8	4.9901 (61)	0.11460 (31)	0.001481 (30)	1.8247 (91)	0.000643 (20)	99.1 ± 0.2	43.7 ± 0.2	198.6 ± 0.8
58287-01I	10	7.9193 (68)	0.18174 (35)	0.002340 (42)	2.9213 (130)	0.001046 (21)	99.0 ± 0.1	43.7 ± 0.1	198.7 ± 0.6
58287-01J	13	9.9026 (78)	0.16265 (36)	0.003924 (54)	2.6180 (102)	0.010361 (38)	71.2 ± 0.2	43.9 ± 0.3	199.5 ± 1.3
58287-01K	20	8.9146 (88)	0.19599 (39)	0.002685 (54)	3.2780 (111)	0.002257 (23)	95.5 ± 0.2	44.0 ± 0.2	199.9 ± 0.7
58287-01L	26	5.3213 (55)	0.11330 (27)	0.001725 (35)	1.8689 (81)	0.001985 (23)	91.8 ± 0.2	43.7 ± 0.2	198.5 ± 0.8
58287-01M	35	4.1691 (49)	0.07178 (23)	0.001656 (29)	1.2137 (83)	0.003956 (26)	74.3 ± 0.2	43.7 ± 0.3	198.7 ± 1.4
NS19 (med.)		*JDisc4 = 0.002664 ± 0.000005 (0.20%)*			*D=1.00654 ± 0.00248*				
58288-01A	2.0	0.5461 (14)	0.01194 (10)	0.000175 (20)	0.1574 (45)	0.000202 (12)	91.4 ± 0.7	42.2 ± 0.5	192.3 ± 2.2
58288-01B	3.0	2.2744 (30)	0.05166 (18)	0.000705 (28)	0.7457 (68)	0.000320 (13)	98.5 ± 0.3	43.8 ± 0.2	199.3 ± 1.0
58288-01C	4.0	4.2027 (47)	0.09598 (26)	0.001268 (27)	1.4379 (100)	0.000530 (15)	99.0 ± 0.2	43.9 ± 0.2	199.3 ± 0.8
58288-01D	4.8	4.0530 (40)	0.09244 (29)	0.001177 (27)	1.3986 (89)	0.000511 (13)	99.0 ± 0.2	43.9 ± 0.2	199.7 ± 0.8
58288-01E	5.5	3.9825 (42)	0.09093 (27)	0.001155 (31)	1.3568 (93)	0.000490 (13)	99.1 ± 0.2	43.9 ± 0.2	199.5 ± 0.8
58288-01F	6.3	3.1841 (35)	0.07300 (24)	0.000957 (25)	1.0594 (77)	0.000360 (13)	99.3 ± 0.2	43.8 ± 0.2	199.1 ± 0.9
58288-01G	7.0	2.5494 (35)	0.05796 (22)	0.000751 (30)	0.8403 (76)	0.000330 (13)	98.8 ± 0.2	43.9 ± 0.2	199.8 ± 1.0
58288-01H	7.8	1.7911 (22)	0.04132 (18)	0.000553 (24)	0.6072 (76)	0.000237 (12)	98.8 ± 0.3	43.3 ± 0.3	197.0 ± 1.1
58288-01I	10	1.6349 (18)	0.03657 (18)	0.000447 (23)	0.5624 (68)	0.000228 (12)	98.6 ± 0.3	44.6 ± 0.3	202.6 ± 1.2
58288-01J	13	1.0743 (19)	0.02503 (17)	0.000340 (22)	0.3818 (54)	0.000134 (12)	99.1 ± 0.4	43.1 ± 0.4	195.9 ± 1.5
58288-01K	20	0.6133 (17)	0.01517 (11)	0.000199 (21)	0.2129 (44)	0.000068 (12)	99.5 ± 0.7	40.7 ± 0.4	185.6 ± 1.8

58288-01L	26	0.5342 (16)	0.01459 (13)	0.000188 (18)	0.1867 (47)	0.000076 (11)	98.6 ± 0.8	36.4 ± 0.4	167.2 ± 1.9
58288-01M	35	0.6773 (17)	0.02172 (12)	0.000289 (20)	0.2183 (44)	0.000102 (11)	98.1 ± 0.6	30.8 ± 0.3	142.4 ± 1.1
NS21		*JDisc4 = 0.002664 ± 0.000005 (0.20%)*			*D=1.00646 ± 0.00238*				
58286-01A	2.0	8.1954 (272)	0.01089 (16)	0.005368 (52)	0.1456 (36)	0.024332 (75)	12.4 ± 0.4	94.3 ± 7.5	404.6 ± 28.6
58286-01B	3.0	1.7011 (78)	0.01524 (13)	0.000902 (26)	0.4265 (52)	0.003491 (28)	41.4 ± 0.7	47.2 ± 1.1	213.6 ± 4.9
58286-01C	4.0	1.0480 (45)	0.02094 (15)	0.000402 (23)	0.7375 (55)	0.000770 (20)	83.9 ± 0.8	43.1 ± 0.5	196.3 ± 2.3
58286-01D	4.8	1.0441 (38)	0.02287 (15)	0.000360 (23)	0.8557 (61)	0.000509 (19)	92.1 ± 0.7	43.3 ± 0.5	196.9 ± 2.0
58286-01E	5.5	1.1623 (37)	0.02599 (16)	0.000444 (26)	1.0140 (90)	0.000438 (19)	95.8 ± 0.7	44.2 ± 0.4	200.7 ± 1.8
58286-01F	6.3	1.3409 (38)	0.03062 (16)	0.000394 (22)	1.1721 (67)	0.000434 (20)	97.4 ± 0.6	43.9 ± 0.4	199.7 ± 1.5
58286-01G	7.0	1.6106 (38)	0.03701 (17)	0.000551 (25)	1.4160 (81)	0.000557 (20)	96.8 ± 0.5	43.4 ± 0.3	197.3 ± 1.3
58286-01H	7.8	1.7499 (38)	0.04010 (18)	0.000547 (25)	1.5639 (87)	0.000499 (20)	98.7 ± 0.5	44.4 ± 0.3	201.7 ± 1.3
58286-01I	10	4.1080 (61)	0.07695 (27)	0.001460 (34)	2.9539 (112)	0.003547 (28)	80.2 ± 0.3	44.1 ± 0.3	200.5 ± 1.3
58286-01J	13	3.3955 (60)	0.07662 (25)	0.001012 (29)	2.8937 (97)	0.001159 (20)	96.7 ± 0.3	44.1 ± 0.2	200.5 ± 1.0
58286-01K	20	6.8490 (60)	0.15527 (36)	0.002065 (38)	5.9575 (141)	0.002050 (23)	98.1 ± 0.2	44.6 ± 0.2	202.4 ± 0.7
58286-01L	26	5.4622 (59)	0.12344 (31)	0.001769 (36)	4.7559 (132)	0.001810 (23)	97.2 ± 0.2	44.3 ± 0.2	201.2 ± 0.8
58286-01M	35	3.3272 (54)	0.07091 (22)	0.001108 (31)	2.7530 (122)	0.001654 (21)	91.9 ± 0.3	44.4 ± 0.2	201.9 ± 1.0
NS23 (coarse)		*JDisc4 = 0.002664 ± 0.000005 (0.20%)*			*D=1.00646 ± 0.00238*				
58290-01A	2.0	0.3747 (38)	0.00968 (15)	0.000418 (30)	0.0852 (38)	0.000337 (20)	75.3 ± 2.0	29.3 ± 0.9	135.7 ± 4.0
58290-01B	3.0	1.2960 (43)	0.03359 (33)	0.002091 (101)	0.4657 (53)	0.001082 (36)	78.2 ± 0.9	30.5 ± 0.5	140.9 ± 2.2
58290-01C	4.0	2.9860 (50)	0.07122 (38)	0.002616 (121)	1.1482 (63)	0.001114 (32)	92.0 ± 0.4	39.1 ± 0.3	178.7 ± 1.3
58290-01D	4.8	3.3048 (55)	0.07656 (26)	0.001406 (40)	1.2864 (62)	0.000558 (21)	98.1 ± 0.3	42.9 ± 0.2	195.3 ± 0.9
58290-01E	5.5	3.6490 (48)	0.08436 (25)	0.001149 (30)	1.3820 (82)	0.000481 (20)	99.1 ± 0.2	43.4 ± 0.2	197.5 ± 0.8
58290-01F	6.3	4.0125 (54)	0.09247 (31)	0.001207 (31)	1.5470 (74)	0.000533 (20)	99.2 ± 0.2	43.6 ± 0.2	198.2 ± 0.9
58290-01G	7.0	3.8931 (53)	0.08992 (26)	0.001146 (28)	1.4860 (88)	0.000523 (20)	99.1 ± 0.2	43.4 ± 0.2	197.6 ± 0.8
58290-01H	7.8	3.4748 (50)	0.08019 (25)	0.001065 (29)	1.3478 (78)	0.000447 (20)	99.3 ± 0.3	43.6 ± 0.2	198.2 ± 0.9
58290-01I	10	5.2589 (51)	0.12143 (31)	0.001659 (36)	2.0469 (83)	0.000727 (20)	99.0 ± 0.2	43.4 ± 0.2	197.6 ± 0.7
58290-01J	13	4.4771 (50)	0.10226 (32)	0.001418 (34)	1.7557 (82)	0.000764 (20)	98.1 ± 0.2	43.5 ± 0.2	197.9 ± 0.8
58290-01K	20	3.0205 (46)	0.07107 (22)	0.000850 (26)	1.2363 (72)	0.000501 (19)	98.4 ± 0.3	42.4 ± 0.2	193.0 ± 0.9
58290-01L	26	2.6126 (46)	0.06442 (24)	0.000873 (27)	1.0917 (60)	0.000389 (20)	98.9 ± 0.3	40.6 ± 0.2	185.5 ± 1.0
58290-01M	35	2.9356 (46)	0.09637 (28)	0.001360 (28)	1.0454 (72)	0.000810 (20)	94.7 ± 0.3	29.1 ± 0.1	134.6 ± 0.6
58287-01A	2	0.3976 (31)	0.01170 (12)	0.000247 (22)	0.0633 (32)	0.000348 (19)	75.4 ± 1.7	25.7 ± 0.6	119.7 ± 2.8
NS23 (med.)		*JDisc4 = 0.002664 ± 0.000005 (0.20%)*			*D=1.00654 ± 0.00248*				
58289-01A	2.0	0.3657 (14)	0.00733 (9)	0.000087 (18)	0.1011 (41)	0.000157 (12)	89.5 ± 1.1	45.2 ± 0.8	205.0 ± 3.5
58289-01B	3.0	1.5544 (31)	0.03527 (15)	0.000459 (25)	0.5913 (58)	0.000275 (12)	97.8 ± 0.4	43.7 ± 0.3	198.5 ± 1.1
58289-01C	4.0	3.3178 (43)	0.07552 (26)	0.000935 (25)	1.3199 (115)	0.000480 (13)	98.9 ± 0.2	44.0 ± 0.2	200.1 ± 0.9
58289-01D	4.8	3.8698 (41)	0.08885 (28)	0.001113 (29)	1.5746 (94)	0.000506 (13)	99.4 ± 0.2	43.9 ± 0.2	199.5 ± 0.8
58289-01E	5.5	3.9719 (38)	0.09097 (23)	0.001110 (30)	1.6106 (111)	0.000517 (13)	99.4 ± 0.2	44.0 ± 0.2	199.9 ± 0.7
58289-01F	6.3	3.8270 (39)	0.08785 (25)	0.001130 (30)	1.5565 (100)	0.000523 (13)	99.2 ± 0.2	43.8 ± 0.2	199.2 ± 0.8
58289-01G	7.0	3.5166 (38)	0.08038 (24)	0.001054 (31)	1.4466 (97)	0.000500 (13)	99.1 ± 0.2	43.9 ± 0.2	199.8 ± 0.8
58289-01H	7.8	2.7959 (35)	0.06361 (21)	0.000890 (27)	1.1636 (85)	0.000391 (13)	99.2 ± 0.2	44.2 ± 0.2	200.9 ± 0.9
58289-01I	10	2.7042 (35)	0.06224 (23)	0.000739 (25)	1.1465 (87)	0.000388 (13)	99.1 ± 0.2	43.7 ± 0.2	198.6 ± 1.0
58289-01J	13	2.2238 (31)	0.05075 (21)	0.000670 (24)	0.9295 (77)	0.000339 (13)	98.8 ± 0.3	43.9 ± 0.2	199.6 ± 1.1
58289-01K	20	1.6451 (20)	0.03724 (18)	0.000492 (23)	0.7165 (83)	0.000259 (12)	98.8 ± 0.3	44.3 ± 0.3	201.3 ± 1.2
58289-01L	26	1.3493 (17)	0.03081 (17)	0.000408 (22)	0.5826 (77)	0.000219 (12)	98.6 ± 0.3	43.8 ± 0.3	199.2 ± 1.3
58289-01M	35	1.2010 (18)	0.02677 (12)	0.000376 (21)	0.5092 (56)	0.000312 (13)	95.7 ± 0.4	43.6 ± 0.3	198.1 ± 1.2

Label	Na_2O (wt%)	MgO	Al_2O_3	SiO_2	K_20	Ca0	$Ti0_2$	MnO	FeO
HB1 PLG5	0.7009	0.934	32.4344	47.9775	9.9863	0.2047	<0.001	0.0771	1.4729
HB1 PLG5	2.8205	0.4255	29.9308	52.4482	8.064	0.652	0.0016	0.0051	1.7746
HB1 PLG5	3.1166	0.4107	30.267	51.4691	7.7139	0.7026	0.0324	0.0508	1.1377
HB1 PLG3	3.8066	0.4753	29.2274	53.9493	6.9908	0.6881	0.0205	0.0284	1.2441
HB1 PLG5	1.7908	5.596	25.4251	44.5835	5.6086	0.3439	0.0556	0.2075	10.0017
HB1 PLG5	2.1522	6.0655	23.8852	44.5919	3.8976	0.4941	0.0115	0.2751	11.4994
HB1 PLG1	6.4649	0.5035	24.9495	58.5641	3.7575	1.121	0.0387	<0.001	1.3447
AN504 PLG1 R-R2_20	1.5268	4.0589	8.4217	62.5377	2.6359	2.1763	1.8107	0.1357	8.0434
HB1 PLG4	7.8129	0.3928	23.4888	61.2526	2.5806	1.6209	0.0426	0.0071	1.5594

Annexe 3: Jourdan et al.

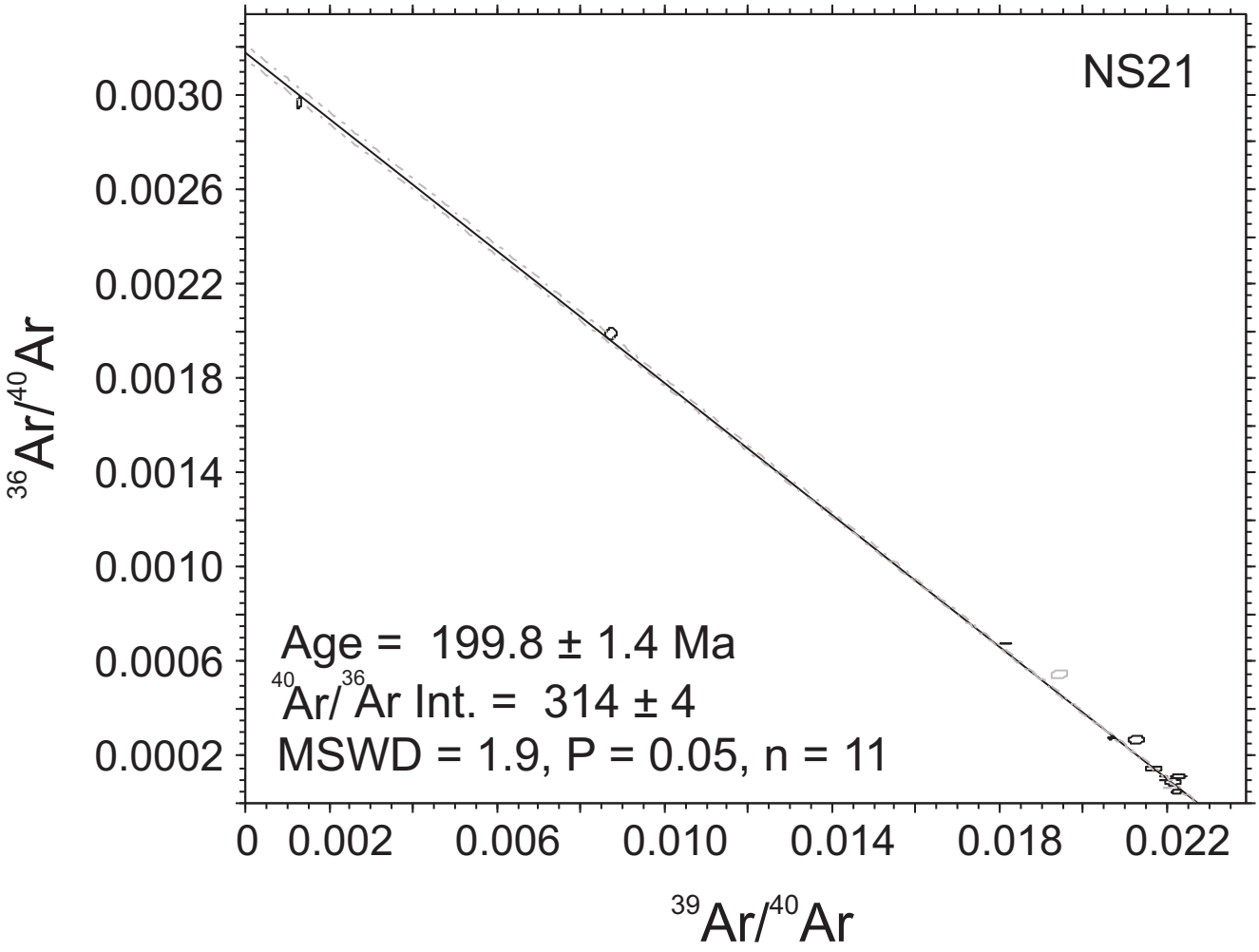

Jourdan et al.: Annexe 4